



**Raytheon**

# **CLOUD TOP PARAMETERS**

## **VISIBLE/INFRARED IMAGER/RADIOMETER SUITE**

### **ALGORITHM THEORETICAL BASIS DOCUMENT**

**Version 4: May 2001**

*Allen Huang*  
*Weather Or Knot*

*Glenn Higgins*  
*Adrian George*

RAYTHEON SYSTEMS COMPANY  
Information Technology and Scientific Services  
4400 Forbes Boulevard  
Lanham, MD 20706

SBRS Document #: Y2395



---

## EDR: Cloud Top Parameters

Doc No: Y2395

Version: 4

Revision: 0

	FUNCTION	NAME	SIGNATURE	DATE
Prepared By	EDR Developer	A. HUANG		5/3/01
Approved By	Relevant Lead	R. SLONAKER		5/13/01
Approved By	Chief Scientist	S. MILLER		5/14/01
Released By	Algorithm Lead	P. KEALY		5/15/01



## TABLE OF CONTENTS

	<u>Page</u>
LIST OF FIGURES .....	iii
LIST OF TABLES .....	v
GLOSSARY OF ACRONYMS .....	vi
DEFINITION OF SYMBOLS .....	vii
ABSTRACT .....	ix
1.0 INTRODUCTION .....	10
1.1 PURPOSE .....	10
1.2 SCOPE .....	10
1.3 VIIRS DOCUMENTS .....	10
1.4 REVISION .....	10
2.0 EXPERIMENT OVERVIEW .....	12
2.1 OBJECTIVES OF CLOUD TOP PARAMETER RETRIEVALS .....	12
2.1.1 Cloud Top Height .....	12
2.1.2 Cloud Top Pressure .....	13
2.1.3 Cloud Top Temperature .....	14
2.2 INSTRUMENT CHARACTERISTICS .....	15
2.3 RETRIEVAL STRATEGY .....	16
3.0 ALGORITHM DESCRIPTION .....	18
3.1 PROCESSING OUTLINE .....	18
3.1.1 General Approach .....	18
3.1.2 UCLA Algorithm for Retrieval of IR Cirrus and Water Cloud Top Temperature .....	19
3.1.3 Window IR Algorithm for Retrieval of Water Droplet Cloud Top Height .....	19
3.1.4 Cloud Top Parameter Interpolation Algorithm .....	20
3.1.5 Alternative and Complementary Algorithms .....	21
3.2 ALGORITHM INPUT .....	21
3.3 THEORETICAL DESCRIPTION OF THE CLOUD TOP PARAMETER RETRIEVAL ALGORITHMS .....	21
3.3.1 Physics of the Problem .....	21
3.3.2 Mathematical Description of the Algorithms .....	24
3.3.3 Archived Algorithm Output .....	26

3.3.4	Variance and Uncertainty Estimates .....	27
3.3.5	Error Budget.....	29
3.4	ALGORITHM SENSITIVITY STUDIES .....	29
3.4.1	Calibration Errors.....	29
3.4.2	Instrument Noise .....	35
3.4.3	Ancillary Data .....	43
3.5	PRACTICAL CONSIDERATIONS.....	43
3.5.1	Numerical Computation Considerations.....	43
3.5.2	Programming and Procedural Considerations.....	44
3.5.3	Configuration of Retrievals.....	44
3.5.4	Quality Assessment and Diagnostics .....	45
3.5.5	Exception Handling.....	46
3.6	ALGORITHM VALIDATION.....	47
3.7	ALGORITHM DEVELOPMENT SCHEDULE .....	48
4.0	ASSUMPTIONS AND LIMITATIONS .....	49
4.1	ASSUMPTIONS.....	49
4.2	LIMITATIONS .....	49
5.0	REFERENCES .....	51

## LIST OF FIGURES

	<u>Page</u>
Figure 1. High-level data flow for cloud top parameter retrieval.....	18
Figure 2. Window IR cloud top height retrieval algorithm. ....	20
Figure 3. Atmospheric layer construction and notional characterization of the optical depth profile. Symbols are defined in the Definition of Symbols table at the beginning of the document. ....	24
Figure 4. Notation used to define vertical structure. ....	26
Figure 5a. Radiometric Accuracy results for 0.1% (top) and 0.5% (bottom) perturbations in the 10.8 $\mu\text{m}$ radiances using Scenario 4 and the Window IR algorithm. The measurement accuracy metric is plotted.....	31
Figure 5b. Radiometric Accuracy results for 1% (top) and 2% (bottom) perturbations in the 10.8 $\mu\text{m}$ radiances using Scenario 4 and the Window IR algorithm. The measurement accuracy metric is plotted.....	32
Figure 6. Radiometric Stability results for 0.1% (top) and 0.5% (bottom) perturbations of the 10.8 $\mu\text{m}$ radiances using Scenario 4 and the Window IR algorithm. The long-term stability metric is plotted. ....	34
Figure 7a. Instrument noise contour plot for measurement accuracy. Scenario 4, Model 1. ....	37
Figure 7b. Instrument noise contour plot for measurement accuracy. Scenario 4, Model 2. ....	37
Figure 7c. Instrument noise contour plot for measurement accuracy. Scenario 4, Model 3. ....	38
Figure 7d. Instrument noise contour plot for measurement accuracy. Scenario 4, Model 4. ....	38
Figure 7e. Instrument noise contour plot for measurement accuracy. Scenario 4, Model 5. ....	39
Figure 7f. Instrument noise contour plot for measurement accuracy. Scenario 4, Model 6. ....	39
Figure 8a. Instrument noise measurement precision. Scenario 4, Model 1.....	40
Figure 8b. Instrument noise measurement precision. Scenario 4, Model 2. ....	40
Figure 8c. Instrument noise measurement precision. Scenario 4, Model 3.....	41
Figure 8d. Instrument noise measurement precision. Scenario 4, Model 4. ....	41
Figure 8e. Instrument noise measurement precision. Scenario 4, Model 5.....	42
Figure 8f. Instrument noise measurement precision. Scenario 4, Model 6. ....	42

Figure 9. Instrument Noise Measurement Precision Results. Scenario 2. ....	43
--	----



## LIST OF TABLES

	<u>Page</u>
Table 1. SRD Requirements for Cloud Top Height .....	13
Table 3. SRD Requirements for Cloud Top Temperature.....	15
*Applies at nadir for fine resolution product. ....	15
Table 4. Bands Used for Cloud Top Parameter Retrievals. An “x” denotes cloud algorithms that use the band. For algorithms other than cloud top parameters, the band list is not necessarily complete. ....	16
Table 5. Description of the Input Data Required by the Cloud Top Parameter Retrieval Algorithms.....	22
Table 6. Major Contributions to Measurement Error.....	28
Table 7. Bias values (in percent) above which threshold measurement accuracy is exceeded for water droplet clouds, with $r_e = 5$ and for $\tau = 1$ and 10. ....	33
Table 8. Bias values (in percent) above which threshold long-term stability is exceeded for water droplet clouds with $r_e = 5$ and for $\tau = 1$ and 10. ....	33
Table 9. Noise model above which threshold measurement precision is exceeded for water droplet clouds with $r_e = 5$ and for $\tau = 1$ and 10.....	36
Table 10. Cloud Top Parameter Retrieval Procedure.....	44
Table 11. Data used by retrieval algorithms, whether the data are essential or nonessential, and primary, secondary, and tertiary data sources. ....	47

## GLOSSARY OF ACRONYMS

ATBD	Algorithm Theoretical Basis Document
AVHRR	Advanced Very High Resolution Radiometer
CLW	Cloud Liquid Water
CMIS	Conical Scanning Microwave Imager/Sounder
CrIS	Cross-track Infrared Sounder
CSSM	Cloud Scene Simulation Model
DISORT	Discrete Ordinate Radiative Transfer
EDR	Environmental Data Record
IPT	Integrated Product Team
IR	Infrared
IWC	Ice Water Content
LOS	Line-of-Sight
MAS	MODIS Airborne Simulator
MODIS	Moderate Resolution Imaging Spectroradiometer
MODTRAN	Moderate Resolution Atmospheric Radiance and Transmittance Model
NPOESS	National Polar-orbiting Operational Environmental Satellite System
RSBR	Raytheon Santa Barbara Research
RSS	Root Sum Square
SNR	Sensor Signal-to-Noise Ratio
SRD	Sensor Requirements Document
TASC	TASC, a division of Litton
TOA	Top of the Atmosphere
VIIRS	Visible/Infrared Imager/Radiometer Suite

## DEFINITION OF SYMBOLS

$z_{cb}$ (km - kilometers)	Cloud Base Height
$r_e$ ( $\mu\text{m}$ or $\text{um}$ (in figures) – micrometers)	Cloud Mean Effective Particle Radius
$D_e$ ( $\mu\text{m}$ - micrometers)	Cloud Mean Effective Particle Size (diameter)
$\tau$ (unitless)	Cloud Optical Depth
$z$ (km - kilometers)	Height
$z_{cb}$ (km - kilometers)	Cloud Base Height
$z_{ct}$ (km - kilometers)	Cloud Top Height
$p$ (mb - millibars)	Pressure
$p_{ct}$ (mb - millibars)	Cloud Top Pressure
$T_{cb}$ (K - degrees Kelvin)	Cloud Base Temperature
$T_{ct}$ (K - degrees Kelvin)	Cloud Top Temperature
$\mu_0$	Cosine of Solar Zenith Angle
$\mu$	Cosine of Sensor Zenith Angle
$I$	Radiance
$\Delta\phi$ (angular degrees)	Sun-Sensor Relative Azimuth Angle
$\phi$ (angular degrees)	Sensor Azimuth Angle
$\theta$ (angular degrees)	Sensor Zenith Angle
$\phi_0$ (angular degrees)	Solar Azimuth Angle
$\theta_0$ (angular degrees)	Solar Zenith Angle
$\lambda$	Wavelength



## ABSTRACT

The Visible/Infrared Imager/Radiometer Suite (VIIRS) Cloud Top Parameters Algorithm estimates cloud top temperature, pressure, and height using VIIRS radiances, other VIIRS Cloud Environmental Data Records (EDR), derived quantities (e.g., cloud mask and phase), and scenario parameters (sun/sensor geometry, atmospheric scenario, etc.). Three retrieval algorithms are used to determine cloud top parameters: The Window Infrared (IR) Algorithm is used during daytime to compute cloud top height using radiance measurements in the 10.8  $\mu\text{m}$  band and radiative transfer analysis with the scenario parameters. It may be applicable at night as well for optically thick water clouds (which is typically the case). The window IR algorithm has a heritage from International Satellite Cloud Climatology Program (ISCCP) which uses 10.8  $\mu\text{m}$  channel to derive cloud top temperature under opaque cloudy condition. Cloud top temperature is derived from not only accounting for the satellite zenith angle but also cloud optical thickness for less opaque cloud (optical thickness smaller than 4.5). The adjusted cloud top pressure that corresponds to cloud top temperature is found from the temperature profile (Rossow, et al., 1991). The algorithm derives cloud top height ( $z_{\text{ct}}$ ) and an Interpolation Algorithm uses  $z_{\text{ct}}$  together with sounding data to determine cloud top temperature ( $T_{\text{ct}}$ ) and cloud top pressure ( $p_{\text{ct}}$ ). The UCLA IR Cirrus Parameter Retrieval Algorithm (see also Ou *et al.*, 2000) computes  $T_{\text{ct}}$  as well as cloud effective particle size and optical depth for cirrus clouds both day and night. The UCLA IR Water Cloud Parameter Retrieval Algorithm (see also Ou *et al.*, 2000) computes  $T_{\text{ct}}$  as well as cloud effective particle size and optical depth for cirrus clouds both day and night. The Interpolation Algorithm uses  $T_{\text{ct}}$  as determined by the UCLA algorithm, together with sounding data, to determine  $z_{\text{ct}}$  and  $p_{\text{ct}}$ .

The UCLA IR Cirrus and Water Cloud Parameter Retrieval Algorithms are described in detail in Ou *et al.* (2000). The TASC Window IR Algorithm and the Cloud Top Parameter Interpolation Algorithm are described in detail in this report. Comments are also made concerning potential alternative or complementary algorithms to retrieve cloud top parameters. In addition, this report provides a description of data flow, the retrieval algorithms and their physical basis, flowdown and sensitivity studies, and algorithm implementation considerations. Measurement requirements for cloud top parameters are specified in the VIIRS Sensor Requirements Document (SRD) and are repeated in this report. TASC Window IR algorithm cloud top parameters performance analysis has been conducted and current simulation result is projected to meet the threshold requirement. Further improvement of algorithm and its validation will be conducted during phase II study period. The algorithm and processing enhancement will be reported in version 5 ATBD.

## 1.0 INTRODUCTION

### 1.1 PURPOSE

This document describes algorithms that will be used to retrieve cloud top parameters using data from the prospective Visible/Infrared Imager/Radiometer Suite (VIIRS) instrument. A description is provided of data flow, the retrieval algorithms and their physical basis, flowdown, EDR performances and sensitivity studies, and implementation considerations. Measurement requirements for cloud top parameters, including cloud top temperature, pressure, and height, are identified in the VIIRS Sensor Requirements Document (SRD).

### 1.2 SCOPE

This document focuses on the theoretical basis for retrieval of cloud top temperature, pressure, and height using VIIRS data. Because multiple algorithms are used for cloud parameter retrieval (i.e., retrieval of cloud optical depth, effective particle size, base height, and amount/layers) and because these parameters are related to the cloud top parameters, frequent reference is made to the other cloud parameter Algorithm Theoretical Basis Documents (ATBDs). In addition, some algorithms estimate multiple parameters, including cloud top temperature. The details of these algorithms are not repeated here; instead, the appropriate ATBD is referenced.

The document is organized into five major sections. The first section is an introduction. The next section provides an overview of the retrieval algorithms, including objectives, instrument characteristics, and retrieval strategy. Section 3 describes the retrieval algorithms and their physical basis, data requirements and issues, algorithm sensitivities to input and flowdown, error budget, practical considerations, validation, and a development schedule. Section 4 provides a brief description of major algorithm assumptions and limitations, and Section 5 is a list of references cited.

### 1.3 VIIRS DOCUMENTS

Visible/Infrared Imager/Radiometer Suite (VIIRS) Sensor Requirements Document (SRD) for National Polar-orbiting Operational Environmental Satellite System (NPOESS) Spacecraft and Sensors. Associate Directorate for Acquisition NPOESS Integrated Program Office. Version 2, Revision a, 4 November 1999. F04701-97-C-0028.

### 1.4 REVISION

This is the fourth revision of this document, dated May 2001.



## 2.0 EXPERIMENT OVERVIEW

This section contains three major subsections. Subsection 2.1 describes the objectives of the cloud top parameter retrievals. Subsection 2.2 describes the characteristics of the VIIRS instrument. Subsection 2.3 addresses the cloud top parameter retrieval strategy.

### 2.1 OBJECTIVES OF CLOUD TOP PARAMETER RETRIEVALS

The cloud top parameter retrieval algorithms, together with the prospective VIIRS sensor, will be developed to meet SRD requirements for cloud top temperature, pressure, and height. For reference, these requirements are provided in Sections 2.1.1 through 2.1.3. Under the VIIRS sensor/algorithm development concept, these requirements are “flowed down” to the design of the most cost-effective sensor/algorithm solution that meets the SRD requirements. This is accomplished through a series of flowdown tests and error budget analyses, which effectively simulate sensor and algorithm performance over a range of environmental and operational scenarios. The error budgets are briefly described in Section 3.3 and described in much more detail in the Raytheon VIIRS Error Budget, Version 3 (Y3249).

#### 2.1.1 Cloud Top Height

The SRD provides the following definition for Cloud Top Height:

*“Cloud top height is defined for each cloud-covered Earth location as the set of heights of the tops of the cloud layers overlying the location. The reported heights are horizontal spatial averages over a cell, i.e., a square region of the Earth’s surface. If a cloud layer does not extend over an entire cell, the spatial average is limited to the portion of the cell that is covered by the layer. Cloud Top height is not defined or reported for cells that are clear. As a threshold, only the height at the top of the highest altitude cloud layer is required. The objective is to report the cloud top height for all distinct cloud layers. This EDR must be generated as a dual product at two spatial scales, one meeting the moderate HCS requirements and the other meeting the fine HCS requirements. The moderate HCS product is the operational requirement, and the fine HCS product is for augmented applications only.”*

Table 1 summarizes the SRD requirements for this parameter.



**Table 1. SRD Requirements for Cloud Top Height**

Para. No.		Thresholds	Objectives
	a. Horizontal Cell Size		
V40.4.7-12	1. Moderate, worst case	25 km	10 km
V40.4.7-13	2. Fine, at nadir	5 km (TBR)	(TBD)
V40.4.7-2	b. Horizontal Reporting Interval	(TBD)	(TBD)
V40.4.7-3	c. Horizontal Coverage	Global	Global
	d. Vertical Cell Size	N/A	N/A
V40.4.7-4	e. Vertical Reporting Interval	Top of highest cloud layer	Top of all distinct cloud layers
V40.4.7-5	f. Measurement Range	0 - 20 km	(TBD)
	g. Measurement Accuracy (moderate HCS product)		
V40.4.7-6	1. Cloud layer optical thickness > 0.1(TBR)	1.0 km (TBR)	0.3 km
V40.4.7-7	2. Cloud layer optical thickness ≤ 0.1(TBR)	2 km	0.3 km
V40.4.7-8	h. Measurement Precision (moderate HCS product)	0.3 km	0.15 km
V40.4.7-14	n. Measurement Uncertainty (fine HCS product)		
V40.4.7-15	1. Water clouds	0.5 km (TBR)*	
V40.4.7-16	2. Ice clouds	1 km (TBR)*	
V40.4.7-9	i. Long-term Stability	0.2 km	0.1 km
V40.4.7-10	j. Mapping Uncertainty	4 km	1 km
	k. Maximum Local Average Revisit Time	8 hrs	6 hrs
	l. Maximum Local Refresh	(TBD)	(TBD)
V40.4.7-11	m. Minimum Swath Width (All other EDR thresholds met)	3000 km (TBR)	(TBD)

\*Applies at nadir for fine resolution product.

## 2.1.2 Cloud Top Pressure

The SRD provides the following definition for Cloud Top Pressure:

*“Cloud top pressure is defined for each cloud-covered Earth location as the set of atmospheric pressures at the tops of the cloud layers overlying the location. The reported pressures are horizontal spatial averages over a cell, i.e., a square region of the Earth’s surface. If a cloud layer does not extend over an entire cell, the spatial average is limited to the portion of the cell that is covered by the layer. Cloud Top pressure is not defined or reported for cells that are clear. As a threshold, only the pressure at the top of the highest altitude cloud layer is required. The objective is to report the cloud top pressure for all distinct cloud layers. This EDR must be generated as a dual product at two spatial scales, one meeting the moderate HCS requirements and the other meeting the fine HCS requirements. The moderate HCS product is the operational requirement, and the fine HCS product is for augmented applications only.”*

Table 2 summarizes the SRD requirements for this parameter.

Table 2. SRD Requirements for Cloud Top Pressure

Para. No.		Thresholds	Objectives
	a. Horizontal Cell Size		
V40.4.8-16	1. Moderate, worst case	25 km	10 km
V40.4.8-17	2. Fine, at nadir	5 km (TBR)	(TBD)
V40.4.8-2	b. Horizontal Reporting Interval	(TBD)	(TBD)
V40.4.8-3	c. Horizontal Coverage	Global	Global
V40.4.8-4	d. Measurement Range	50 – 1050 mb	(TBD)
	e. Measurement Accuracy (moderate HCS product)		
V40.4.8-5	1. Surface - 3 km	100 mb	30 mb
V40.4.8-6	2. 3 - 7 km	75 mb	22 mb
V40.4.8-7	3. > 7 km	50 mb	15 mb
	f. Measurement Precision (moderate HCS product)		
V40.4.8-8	1. Surface - 3 km	50 mb	10 mb
V40.4.8-9	2. 3 - 7 km	38 mb	7 mb
V40.4.8-10	3. > 7 km	25 mb	5 mb
V40.4.8-18	l. Measurement Uncertainty (fine HCS product) (for any altitude or pressure)	50 mb (TBR)*	(TBD)
	g. Long-term Stability		
V40.4.8-11	1. Surface - 3 km	10 mb (TBR)	3 mb
V40.4.8-12	2. 3 - 7 km	7 mb (TBR)	2 mb
V40.4.8-13	3. > 7 km	5 mb (TBR)	1 mb
V40.4.8-14	h. Mapping Uncertainty	4 km	1 km
	i. Maximum Local Average Revisit Time	8 hrs	3 hrs
	j. Maximum Local Refresh	(TBD)	(TBD)
V40.4.8-15	k. Minimum Swath Width (All other EDR thresholds met)	3000 km (TBR)	(TBD)

\*Applies at nadir for fine resolution product.

### 2.1.3 Cloud Top Temperature

The SRD provides the following definition for Cloud Top Temperature:

*“Cloud Top temperature is defined for each cloud-covered Earth location as the set of atmospheric temperatures at the tops of the cloud layers overlying the location. The reported temperatures are horizontal spatial averages over a cell, i.e., a square region of the Earth’s surface. If a cloud layer does not extend over an entire cell, the spatial average is limited to the portion of the cell that is covered by the layer. Cloud Top temperature is not defined or reported for cells that are clear. As a threshold, only the temperature at the top of the highest altitude cloud layer is required. The objective is to report the cloud top temperature for all distinct cloud layers. This EDR must be*

*generated as a dual product at two spatial scales, one meeting the moderate HCS requirements and the other meeting the fine HCS requirements. The moderate HCS product is the operational requirement, and the fine HCS product is for augmented applications only.”*

Table 3 summarizes the SRD requirements for this parameter.

**Table 3. SRD Requirements for Cloud Top Temperature**

Para. No.		Thresholds	Objectives
	a. Horizontal Cell Size		
V40.4.9-13	1. Moderate, worst case	25 km	10 km
V40.4.9-14	2. Fine, at nadir	5 km (TBR)	(TBD)
V40.4.9-2	b. Horizontal Reporting Interval	(TBD)	(TBD)
V40.4.9-3	c. Horizontal Coverage	Global	Global
V40.4.9-4	d. Measurement Range	180 - 310 K	(TBD)
	e. Measurement Accuracy (moderate HCS product)		
V40.4.9-5	1. Cloud layer optical thickness > 0.1 (TBR)	3 K	1.5 K
V40.4.9-6	2. Cloud layer optical thickness ≤ 0.1 (TBR)	6 K	(TBD)
V40.4.9-7	f. Measurement Precision (moderate HCS product)	1.5 K	0.5 K
V40.4.9-15	l. Measurement Uncertainty (fine HCS product) (for any cloud layer optical thickness)	5 K (TBR)*	2K
V40.4.9-8	g. Long-term Stability	1 K	0.1 K
V40.4.9-9	h. Mapping Uncertainty	4 km	1 km
	i. Maximum Local Average Revisit Time	6 hrs	6 hrs
	j. Maximum Local Refresh	(TBD)	(TBD)
V40.4.9-12	k. Minimum Swath Width (All other EDR thresholds met)	3000 km (TBR)	(TBD)

\*Applies at nadir for fine resolution product.

## 2.2 INSTRUMENT CHARACTERISTICS

Table 4 provides the wavebands currently being considered for VIIRS cloud top parameter retrieval. As described in more detail below, bands centered at 0.672, 3.70, and 10.76  $\mu\text{m}$  are used for IR cirrus and water cloud parameter retrievals, and the band centered at 10.76  $\mu\text{m}$  is used for the Window IR retrieval of cloud top parameters for water droplet clouds. Note that there have been minor changes to band centers during the course of the project; the changes were driven by other EDRs not clouds. At the time of the previous version of this report, the comparable band centers were 0.645, 3.750, and 10.800  $\mu\text{m}$ . Many of the results in this report were produced using those band centers. We do not expect performance variation for the cloud parameters due to these changes.

The VIIRS sensor will be on board a polar-orbiting platform with nominal spacecraft altitude of 833 km. The scanning pattern will be normal to the satellite ground track with a maximum sensor-viewing angle of approximately 56 degrees off nadir, relative to the spacecraft position. The nominal VIIRS nadir pixel size for each channel is approximately 760m.

**Table 4. Bands Used for Cloud Top Parameter Retrievals. An “x” denotes cloud algorithms that use the band. For algorithms other than cloud top parameters, the band list is not necessarily complete.**

VIIRS Band Number	Center $\lambda$ ( $\mu\text{m}$ )	Band Width ( $\mu\text{m}$ )	Cloud Top Parameters	Cloud Effective Particle Size*	Cloud Optical Depth*	VIIRS Cloud Mask
M5	0.672	0.02	x	x	x	x
M12	3.700	0.18	x	x	x	x
M15	10.763	1.00	x	x	x	x

## 2.3 RETRIEVAL STRATEGY

The cloud top parameter retrieval algorithms will use VIIRS radiance data, other VIIRS cloud data (e.g., pixel-level cloud optical depth, effective particle size, and satellite geometry), internal cloud EDR (VIIRS cloud mask), and ancillary data products. The VIIRS cloud mask will identify whether each VIIRS pixel is clear or cloud-contaminated. The mask will also provide additional information, such as cloud phase (ice, water, mixed, or multilayer). The cloud phase information will be used to determine which of three algorithms will be used to retrieve cloud top parameters: the UCLA IR cirrus parameter retrieval algorithm for ice clouds, the UCLA IR water cloud parameter retrieval algorithm for water clouds during night, or the TASC, a division of Litton (TASC), Window Infrared (IR) algorithm for water droplet clouds during daytime or night. These algorithms are described in more detail in Section 3. The UCLA IR retrieval algorithms retrieve cloud top temperature, effective particle size, and optical depth for cirrus and water clouds. The TASC Window IR algorithm provides cloud top height retrieval for water droplet clouds. Given cloud top temperature or cloud top height, the remaining two cloud top parameters are obtained through the use of an appropriate atmospheric sounding and an interpolation algorithm. At night, both UCLA and TASC water cloud top temperature retrieval will also be intercompared and possible quality control information be generated.



### 3.0 ALGORITHM DESCRIPTION

This section contains six major subsections addressing the cloud top parameter processing flow: algorithm input and output, the algorithm theoretical basis and mathematical description; algorithm sensitivity to inputs and analyses; practical implementation considerations, validation; and algorithm development schedule.

#### 3.1 PROCESSING OUTLINE

##### 3.1.1 General Approach

A high-level flow diagram of the general approach to determining cloud top parameters appears in Figure 1. Input parameters required by the algorithms include pixel-level data from other VIIRS cloud algorithms (optical depth and effective particle size), VIIRS internal EDR (e.g., cloud mask and phase), VIIRS radiances, and scenario parameters (e.g., sun/sensor geometry and atmospheric scenario). The cloud phase along with day/night flag are used to determine whether retrieval will be made by the Window IR algorithm (water clouds during daytime), the UCLA IR Water Cloud Retrieval Algorithm (water clouds during night) or the UCLA IR Cirrus Parameter Retrieval Algorithm (ice clouds day or night). The Window IR Algorithm returns cloud top height ( $z_{ct}$ ) and a Cloud Top Parameter Interpolation Algorithm uses  $z_{ct}$  together with sounding data to determine cloud top temperature ( $T_{ct}$ ) and cloud top pressure ( $p_{ct}$ ). The UCLA IR Cirrus and Water Cloud Parameter Retrieval Algorithms return  $T_{ct}$  and the Cloud Top Parameter Interpolation Algorithm uses  $T_{ct}$ , together with sounding data, to determine  $z_{ct}$  and  $p_{ct}$ . Brief descriptions of the UCLA IR Cirrus and Water Cloud Parameter Retrieval Algorithms, the TASC Window IR Algorithm, and the Interpolation Algorithm follow.

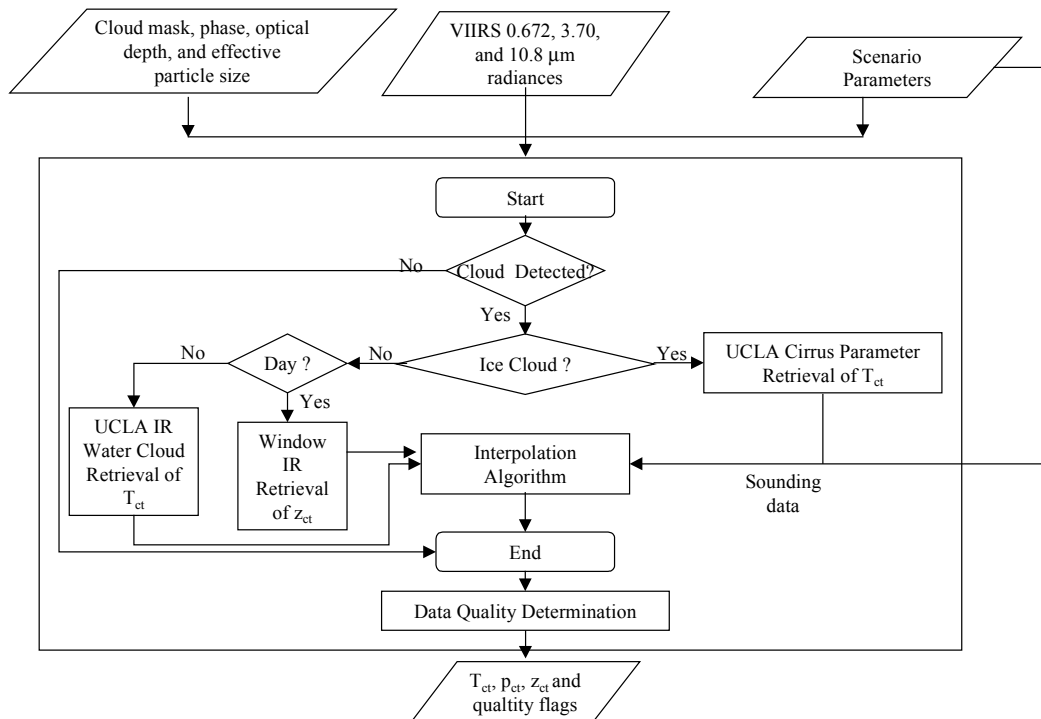


Figure 1. High-level data flow for cloud top parameter retrieval.

### 3.1.2 UCLA Algorithm for Retrieval of IR Cirrus and Water Cloud Top Temperature

The UCLA IR Cirrus Parameter Retrieval Algorithm calculates cloud top temperature using a 2-band (nighttime) or 3-band (daytime) retrieval algorithm. The algorithm also retrieves cirrus cloud effective particle size and emissivity/optical depth. The cloud top height and pressure are obtained by interpolation using an atmospheric sounding and the Cloud Top Parameter Interpolation Algorithm. The IR Water Cloud Parameter Retrieval Algorithm is similar; thus far, it has been applied to nighttime conditions only.

### 3.1.3 Window IR Algorithm for Retrieval of Water Droplet Cloud Top Height

The retrieval of cloud top parameters for water clouds is based on the Window IR technique using 10.8  $\mu\text{m}$  radiances. The approach is depicted in Figure 2. To retrieve the cloud top parameters this algorithm requires as input, a measured 10.8  $\mu\text{m}$  radiance value, the VIIRS Cloud Effective Particle Size Environmental Data Record, the VIIRS Cloud Optical Depth EDR, and an atmospheric temperature and moisture profile. Interpolation on a radiance look-up table retrieves the cloud top altitude. The pressure and temperature EDRs are then obtained by interpolation using sounding data. Initially, flowdown results were generated by running the Moderate Resolution Atmospheric Radiance and Transmittance Model (MODTRAN) over a range of cloud altitudes, effective particle sizes, and optical depths and scenario conditions. We then transitioned to the UCLA Radiative Transfer Model (see Ou *et al.*, 2000). All Error Budget results were produced using the UCLA Radiative Transfer Model.

The sensitivity of cloud top parameter retrievals (e.g., CTT) to EPS and COT generally favors the use of algorithms which can compute all three parameters simultaneously (such as the UCLA IR retrieval algorithms) or can use EPS and COT obtained from other algorithms to augment the cloud top parameter retrieval (such as the Window IR algorithm). It should be noted, however, that the Window IR algorithm can provide accurate results even with uncertain knowledge of COT and EPS, when the “effective” optical depth is large. We define effective optical depth as  $\tau(\text{nadir view}) / \sin(\text{sensor elevation angle}[90 = \text{overhead}, 0 = \text{horizon}])$ . For this reason, the Window IR algorithm is probably appropriate for situations when EPS and COT are not well-known, but when the effective optical depth is large. This generalizes the use of the Window IR to other scenarios, including thick cirrus clouds. For example, when the pixel-level effective blackbody temperature of a cloud is less than about 240K, the cloud is almost certainly a thick ice cloud. In this case, the single-band Window IR algorithm, rather than the two-band UCLA IR algorithm, may be used to determine CTT. This approach may be preferable, in fact, since the calibration error associated with the 3.7  $\mu\text{m}$  band, which use the two-band approach, increases substantially with decreasing BBT. As the calibration error increases, the retrieval error increases. On the other hand, the calibration error associated with the 10.8  $\mu\text{m}$  band is relatively smaller at cold temperatures. Finally, the use of the Window IR algorithm may also improve results at EOS for water clouds during night and ice clouds during both day and night. Even though EPS and COT are less well-known during night, the effective optical depth can be large enough at EOS to make this uncertainty tolerable in most situations.

So far we have assumed all VIIRS cloudy pixels are overcast (100% cloud cover within single VIIRS pixel). For sub-pixel cloudy case (less than 100% cloud cover), during phase II, both UCLA and TASC retrieval algorithm will take into account of this effect and analyze algorithm performance at different view angles (nadir and EOS). The full analysis of sub-pixel cloud effect

will be reported in version 5 ATBD.

VIIRS 10.8  $\mu\text{m}$  band radiance subjects to water vapor continuum absorption. Using 10.8  $\mu\text{m}$  data directly without any prior correction will result under-estimation of cloud top height. Continuum absorption manifests itself in the infrared and millimetre wave window regions of the atmospheric spectrum causing the windows to be less transparent than predicted by molecular absorption alone. For channels designed to be “window” this is obviously an important factor. This continuum absorption/emission has a smooth frequency dependence making it impossible to ascribe to specific molecular transitions. For most of the water cloud, cloud altitude usually is lower and there are lots of moisture exists above the cloud top. Precipitable water above cloud top is one of the new NPOESS EDR and can be conveniently used as an additional input to the TASC window IR algorithm to remove this water vapor absorption on 10.8  $\mu\text{m}$  very effectively.

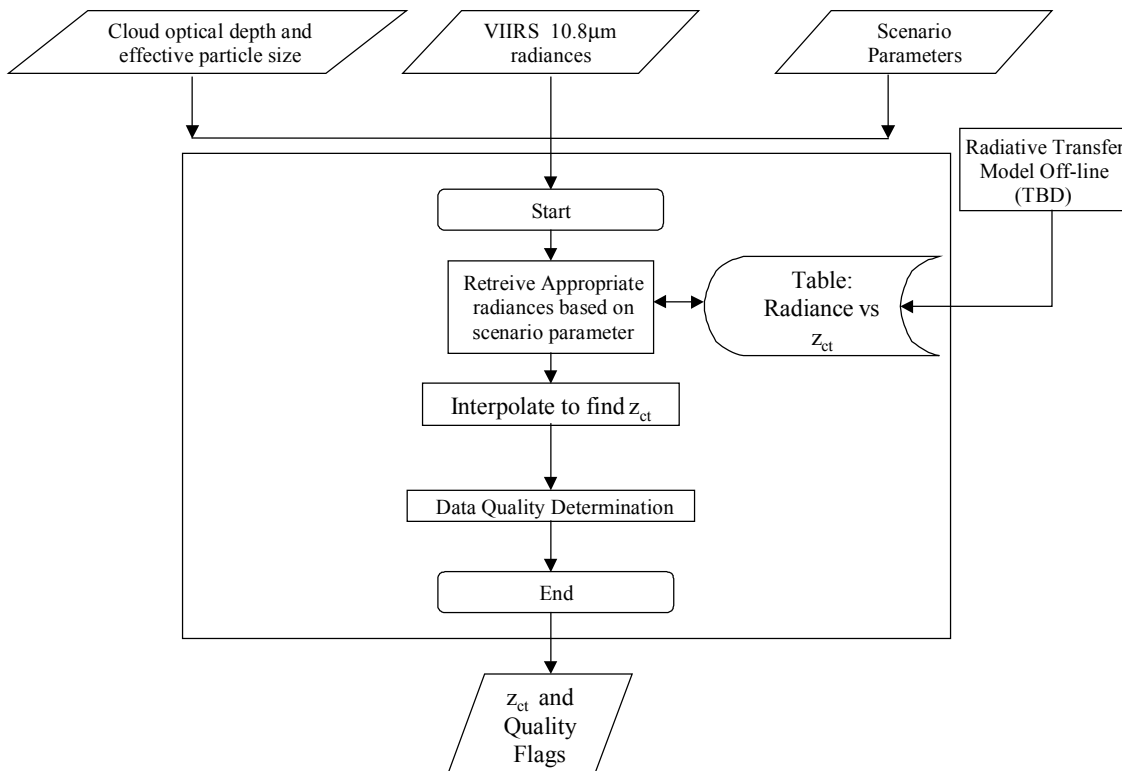


**Figure 2. Window IR cloud top height retrieval algorithm.**

### 3.1.4 Cloud Top Parameter Interpolation Algorithm

Given one of the three cloud top parameters (cloud top temperature, height, or pressure) the other two parameters are determined by interpolation using atmospheric sounding data. The hydrostatic approximation is used to interpolate between pressure levels in the sounding; cloud top temperature and height are obtained via linear interpolation between sounding levels. It is assumed that sounding data are always available, either from archived numerical analyses forecasts, CrIS or the Conical Scanning Microwave Imager/Sounder (CMIS).



### 3.1.5 Alternative and Complementary Algorithms

We did examine the possibility of using the CO<sub>2</sub> channels available from the CrIS to provide coarser resolution (than VIIRS) cirrus cloud top pressure and emissivity information that could complement the UCLA cirrus parameter retrievals. We determined that the UCLA approach, which retrieves cloud optical depth, effective particle size, and cloud top temperature, was capable of meeting SRD requirements. For 25 km HCS, CrIS sensor will provide multiple pixel cloud top parameters at very high accuracy. A possible synergistical alternative and complementary cloud top parameters approach will not only meet threshold but also objective requirement..

## 3.2 ALGORITHM INPUT

Table 5 provides VIIRS and non-VIIRS input data required by the Cloud Top Parameter Algorithms.

## 3.3 THEORETICAL DESCRIPTION OF THE CLOUD TOP PARAMETER RETRIEVAL ALGORITHMS

### 3.3.1 Physics of the Problem

The physics of the UCLA IR Cirrus and Water Cloud Cloud Parameter Retrieval algorithms, which determine effective particle size, optical depth, and cloud top temperature, is described in Ou *et al.* (2000). The discussion here will focus on the Window IR Algorithm, on the determination of cloud top height and pressure given cloud top temperature, and on cloud top pressure and temperature, given cloud top height.

The physical basis of the Window IR Algorithm relies on the following characteristics of the Earth-atmosphere system:

- The radiation reaching the top of the atmosphere in the 10.3 to 11.3  $\mu\text{m}$  region is due primarily to thermal emission by the ground, the atmosphere, and the clouds.
- Optically thick clouds, such as most water droplet clouds, are nearly blackbodies in the long-wave IR portion of the electromagnetic spectrum. Most surface materials have emissivities close to one and are nearly blackbodies as well.
- The atmosphere is nearly transparent in the 10.3 to 11.3  $\mu\text{m}$  region, although some attenuation does occur. Atmospheric attenuation is primarily due to absorption by H<sub>2</sub>O, CO<sub>2</sub>, and aerosols.
- To a reasonable approximation, atmospheric pressure decreases exponentially with height following the hydrostatic equation. Atmospheric temperature decreases monotonically with height in most cases (exceptions being atmospheric inversions in the troposphere and at the tropopause).

**Table 5. Description of the Input Data Required by the Cloud Top Parameter Retrieval Algorithms**

Data Type	Description	Use	Potential Source
VIIRS Radiances	0.670, 3.70, and 10.8 $\mu\text{m}$ radiances	Used to retrieve cloud top properties	VIIRS
Sensor Viewing Geometry	Sensor zenith and azimuth angles for each pixel	Input to radiative transfer model look-up table	Calibrated Radiances SRD
Solar Geometry	Solar zenith and azimuth angles for each pixel	Input to radiative transfer model look-up table and algorithm decision tree	Calibrated Radiances SRD
Cloud Mask	Cloud/no cloud for each pixel	Performed only on cloud-contaminated pixels	VIIRS Cloud Mask algorithm
Cloud Phase	Ice or water cloud flag	Determines which cloud top parameter retrieval algorithm is used	VIIRS Cloud Mask algorithm
Cloud Optical Thickness	Pixel-level optical thickness of water cloud.	Input to radiative transfer model look-up table for Window IR algorithm	VIIRS Cloud Optical Depth algorithm
Cloud Effective Particle Size	Pixel-level effective particle size of water cloud	Input to radiative transfer model look-up table for Window IR algorithm	VIIRS Cloud Effective Particle Size algorithm
Atmospheric Sounding	Atmospheric Temperature and relative humidity as functions of pressure and height	Input to radiative transfer model look-up table and used to infer any two of cloud top height, pressure, and temperature given one of these parameters	NCEP re-analysis and forecast, CrIS sounding data, CMIS sounding data
Surface Emissivity	In-band emissivity of Earth's surface	Input to radiative transfer model look-up table	Emissivity from Spectral Library associated with terrain category database values, e.g., from VIIRS Surface Types-Olson IP
Surface Skin Temperature	Skin temperature associated with pixel region	Input to radiative transfer model look-up table	NCEP re-analysis and forecast, VIIRS Land Surface Temperature EDR and Sea Surface Temperature EDR

As a result of these characteristics of the Earth-atmosphere system in the 10.3 to 11.3  $\mu\text{m}$  region, the radiation reaching the top of the atmosphere (TOA) is strongly affected by cloud layers, when they are present, permitting retrieval of cloud top parameters. Optically thick water droplet clouds are nearly blackbodies, and most of the upwelling radiation at cloud top is from the cloud itself when VIIRS pixel is completely covered by cloud. Little radiation from below the cloud layer reaches the cloud top because it is absorbed by the cloud layer. When optically thick cloud layers are not present, most of the upwelling radiance at the TOA is from the ground. Both the clouds and the ground contribute to the TOA radiance when the clouds are not optically thick; the relative contribution depends on the cloud thickness and effective particle size. The relationship between atmospheric pressure, temperature, and height permits determining cloud top pressure and height, once the cloud top temperature is known, or cloud top pressure and temperature, once cloud top height is known and assuming that an atmospheric temperature

profile is available.

In describing IR radiative transfer mathematically, we use the plane parallel atmospheric approximation as depicted in Figure 3 for a single layer cloud. In the plane parallel atmospheric approximation, it is assumed that variations in atmospheric parameters occur only in the vertical direction. Following Liou (1992), the equation defining monochromatic thermal upwelling intensity at TOA in a plane parallel atmosphere is:

$$I_{\lambda}(\tau^*) = \varepsilon_{\lambda} B_{\lambda}(T_{sfc}) t_{\lambda}(\tau^* / \mu) + \int_0^{\tau^*} B_{\lambda}(\tau') t_{\lambda}(\tau' / \mu) d\tau' / \mu \quad (1)$$

where:

$I_{\lambda}$  = monochromatic radiance

$\tau$  = vertical optical depth

$\tau^*$  = total vertical optical

$\varepsilon_{\lambda}$  = surface emissivity

$\lambda$  = monochromatic wavelength

$B_{\lambda}$  = Planck function

$T_{sfc}$  = skin temperature at Earth's surface

$t_{\lambda}$  = monochromatic transmission =  $e^{-(\tau/\mu)}$

$\mu$  = cosine of sensor viewing angle

For cloudy VIIRS pixel which will measure energy from both clear and cloudy fraction as

$$I_{\lambda} = (1-f\varepsilon_{\lambda,c}) I_{\lambda,clr} + f\varepsilon_{\lambda,c} I_{\lambda,cld} \quad (2)$$

where

$f$  = sub-pixel cloud fraction

$\varepsilon_{\lambda,c}$  = cloud emissivity

$I_{\lambda,clr}$  = clear radiance

$I_{\lambda,cld}$  = opaque cloudy radiance

We'll examine the use of non-overcast cloudy pixel 10.8  $\mu\text{m}$  radiance, which  $f$  is smaller than 1 and cloud emissivity,  $\varepsilon_{\lambda,c}$  is modeled using UCLA cloud parameterization, to analyze the sub-pixel cloud effects on the Window IR cloud height retrieval performance.

Figure 3 provides a notional characterization of the vertical optical depth profile. As depicted

here and as frequently occurs in the atmosphere, the largest contribution to optical depth is from the cloud layer. Because the transmission is typically small in Layers 1 and 2 and because the surface emissivity is close to one in most cases, the primary contribution to the radiance at the top of the atmosphere is from the cloud layer and/or the ground. Note also that the Planck emission depends on temperature as well as wavelength, and so the temperature variation with height, including within the cloud, will affect the radiance intensity at the top of the atmosphere.

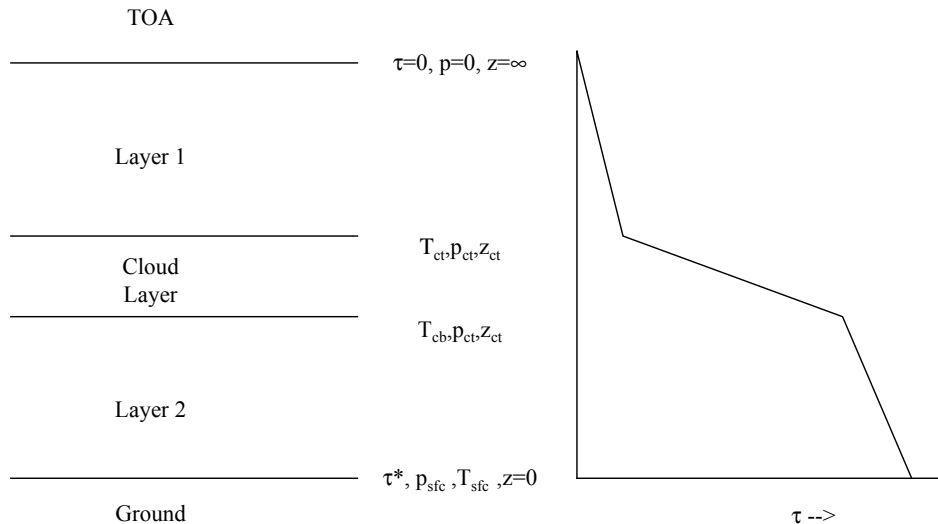


**Figure 3. Atmospheric layer construction and notional characterization of the optical depth profile. Symbols are defined in the Definition of Symbols table at the beginning of the document.**

The thermal emission model depicted in Equation 1 and 2 are generally good approximations in the 10.8  $\mu\text{m}$  region. However, there is some scattering in clouds, even at these wavelengths, and a small contribution to radiance can be expected with multiple scattering within the clouds. For this reason, we have included all effects (thermal emission and multiple scattering) in our simulations and our look-up table solution. We have specified the cloud optical properties, the extinction coefficient, the single scattering albedo, and the asymmetry parameter for water droplet clouds for effective particle sizes ranging from 2 to 32  $\mu\text{m}$  and visible optical depth ranging from 0.05 to 30. These optical property data were obtained from parameterizations of Mie scattering and absorption results developed by Chylek *et al.* (1992). Initially, we used MODTRAN Version 3.7 in the multiple scattering mode using the Discrete Ordinate Radiative Transfer (DISORT) 8-stream. We have since transitioned to the UCLA radiative transfer model (Ou *et al.*, 2000) for all of our work.

### 3.3.2 Mathematical Description of the Algorithms

A discussion of the Window IR algorithm follows. For a detailed description of the UCLA IR cirrus and water cloud parameter retrieval algorithms, the other algorithms used to retrieve cloud top parameters, see Ou *et al.* (2000)

### 3.3.2.1 Window IR Algorithm

To support flowdown studies, we have constructed lookup tables for specific environmental scenarios. These lookup tables contain radiance values as a function of cloud top altitude (for altitudes ranging from 1 km to several kilometers), cloud effective particle size ranging from 2 to 32  $\mu\text{m}$ , and cloud vertical optical thickness (visible) ranging from 0.05 to 30. We have assumed a cloud thickness of 1 km. Given pixel-level effective particle size and optical thickness from other cloud EDR algorithms, we determine cloud top height by linear interpolation in the radiance lookup tables, using an “observed” radiance value for which the cloud top height is unknown.

This setup has sufficed for flowdown studies of sensor parameters, but in routine operations the “environmental scenario” will vary from location to location and from day to day, and is defined from the ancillary data sources identified in Section 3.2. There are two approaches to obtaining the radiance lookup tables for the environmental scenario associated with the observed radiance measurements. The radiance lookup tables can either be pre-computed over a range of values of the ancillary data *or* they can be computed on the fly for the environmental scenario corresponding with the horizontal cell for which EDR values will be reported. Either approach requires trade studies and will be performed during phase II. If pre-computed lookup tables are used, they will need to cover the full operational range of the ancillary input data required by the algorithm. The resolution of the specification of the ancillary data will need to be determined. If the second approach is used, an efficient radiative transfer model will need to be identified and the required computational resources carefully studied.

The specified values of cloud optical depth and effective particle size affect the retrieval of cloud top temperature as described in Subsection 3.4. Because the cloud effective particle size and optical depth algorithms also rely on knowledge of cloud top temperature, it is likely that an iterative approach will be necessary. First-guess values of cloud effective particle size and optical depth will be used initially to retrieve cloud top parameters. The retrieved cloud top parameters will then be used by the cloud effective particle size and optical depth algorithms to retrieve those parameters. Next, the retrieved effective particle size and optical depth values will be used in the cloud top parameter algorithm. This process will again be repeated (probably only a few times) until solutions vary little between successive iterations.

In cases where multi-cloud layers occur, the lower cloud layers will also contribute to the TOA radiances. The effect will be less when the upper cloud is optically thick. Nevertheless, some degradation in performance can be expected in the presence of multilayer cloud systems. For example, the MODIS Cloud Top Properties and Cloud Phase Algorithm Theoretical Basis Document (Menzel and Strabala, 1997, page 27) states that “multilayer cloud situations where an opaque cloud underlies a transmissive cloud cause errors in the height of the transmissive cloud of about 100 mb for most cases.”

### 3.3.2.2 Cloud Top Parameter Interpolation Algorithm

This subsection outlines the processes for determining (1) the cloud top temperature and pressure given height and (2) the cloud top pressure and height given temperature for the sounding scenario depicted in Figure 4, where:

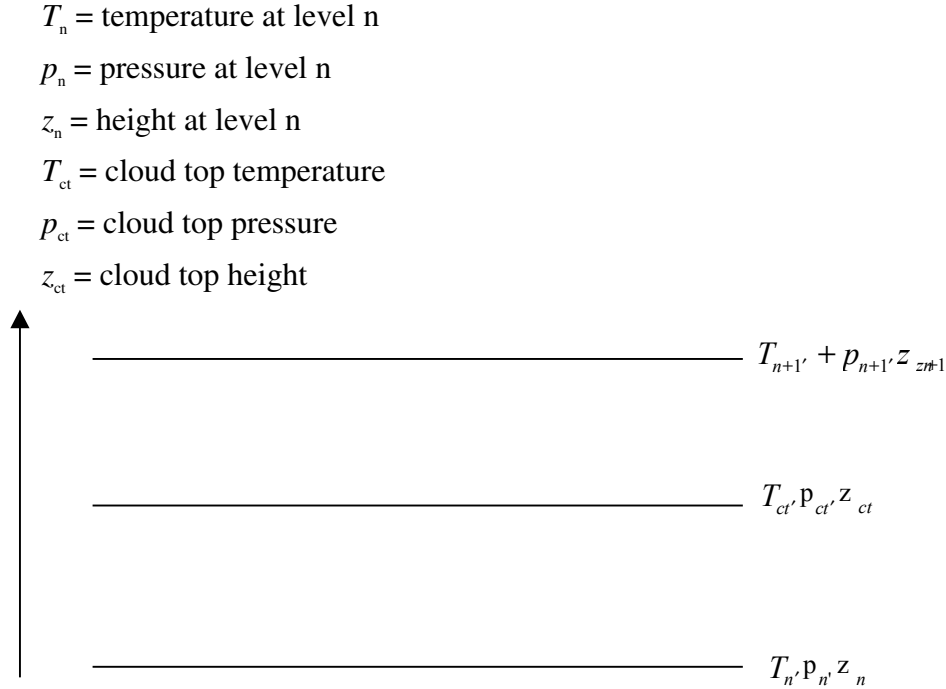


**Figure 4. Notation used to define vertical structure.**

In the case where  $z_{ct}$  is known, then  $T_{ct}$  is determined by linear interpolation between  $T_n$  and  $T_{n+1}$  and  $p_{ct}$  is determined via hydrostatic interpolation in the form

$$p_{ct} = p_n \bullet \exp\left(\frac{g(z_n - z_{ct})}{R\bar{T}}\right) \quad (3)$$

where  $g = .00981 \text{ km/s}^2$ ,  $R$  = gas constant for dry air, and  $\bar{T} = (T_n + T_{ct})/2$ .

In the case where  $T_{ct}$  is known, then  $z_{ct}$  is determined by linear interpolation using the temperature profile between  $z_n$  and  $z_{n+1}$  and  $p_{ct}$  is determined as above.

### 3.3.2.3 Atmospheric Temperature Inversion/Isothermal

The determination of cloud top parameters is more difficult when cloud layers are near atmospheric temperature inversions. In these cases, it is possible that multiple atmospheric layers will have the same temperature, and association of cloud top temperature with a particular atmospheric level may not be possible based only on the radiance measurements. It is possible, however, that the atmospheric structure may provide clues to the probable location of a cloud layer relative to the inversion. The approach to handling inversions should be the subject of future research where high spectral resolution CrIS radiances can provide this inversion or isothermal information.

### 3.3.3 Archived Algorithm Output

The primary output products of the cloud top parameter algorithms are cloud top temperature,

cloud top height, and cloud top pressure. In addition, it is anticipated that a number of data quality flags will be associated with these products. These flags will be implemented in next version software. These flags may address the following:

- Quality of atmospheric sounding (potentially based on the sounding source and associated quality flags).
- Quality of other ancillary input data (e.g, surface temperature, surface emissivity).
- Uncertainty due to the existence of an inversion/isothermal in the temperature profile.
- Uncertainty due to the presence of multilayer clouds using data from the Cloud Cover/Layers (CCL) algorithm.
- Large difference between UCLA and TSAC water cloud height retrieval.
- Other.

### 3.3.4 Variance and Uncertainty Estimates

In this section, the approach used to estimates to determine error budgets for the EDR parameters is described. The total measurement error for a given cloud top parameter can be approximated as follows:

$$E_T^2(M) = \sum E_i^2(M) \quad (4)$$

where:

- $E_T$  = total error of EDR parameter
- $M$  = accuracy or precision Metric
- $E_i$  =  $i^{\text{th}}$  component of error contribution

It is assumed that the individual contributions to total measurement error are independent (uncorrelated).

Note also that:

$$E_T^2(\text{Uncertainty}) = E_T^2(\text{Accuracy}) + E_T^2(\text{Precision})$$

The sensor and ancillary input contributions each have several components. Table 6 captures the major contributions to these measurement error sources.

**Table 6. Major Contributions to Measurement Error**

Error	Error Component	Description
Algorithm	(otherwise referred to as the intrinsic algorithm error)	Retrieval algorithm (model) error assuming perfect sensor and ancillary input data
Sensor	Noise (NEDT)	Sensor noise, assumed to be random, uncorrelated between channels, and uncorrelated spatially
	Modulation Transfer Function (MTF)	Contribution to pixel radiance from outside the pixel.
	Calibration (Absolute Radiometric Accuracy [ARA])	Biases in radiance measurements due to calibration errors; can be due to variations in blackbody emission/reflection sources used for on-board calibration
	Band-to-Band Registration	Relative pointing errors among channels; e.g., channel A looks at a slightly different location than channel B
	Geolocation (mapping)	Uncertainty in knowledge of pixel location
Ancillary Data	Vertical Temperature/Pressure/Moisture profiles	Uncertainty in the knowledge of atmospheric temperature or moisture at one or more levels of the atmosphere. Leads to errors in TOA simulated radiances.
	Surface Emissivity	Uncertainty in the knowledge of surface emissivity. Leads to errors in TOA simulated radiances.
	Surface (skin) Temperature	Uncertainty in the knowledge of surface (skin) temperature. Leads to errors in TOA simulated radiances.
	Effective Particle Size	Uncertainty in the knowledge of effective particle size. Effects the Window IR algorithm.
	Cloud Optical Thickness	Uncertainty in the knowledge of cloud optical thickness. Effects the Window IR algorithm.
	Cloud Mask	Errors in the cloud mask, especially when pixels are identified as cloud-filled when they are actually clear
	Cloud Phase	The cloud top parameters algorithms will err when the cloud phase is incorrectly determined; leading to using the wrong branch in the algorithm

In general, we parameterize the contributions to measurement errors as follows:

$$E_i = \delta x / \delta y \sigma_y \approx \Delta x / \Delta y \sigma_y$$

where:

$x$  =  $M$  metric values for baseline (no noise) case and for EDR parameter (cloud top temperature, pressure, or height) perturbation

$$\Delta x = |x(M) - x(M)_{\text{no noise}}|$$

$y$  = value of error contributor (e.g., skin temperature)

$\Delta y$  = magnitude of the perturbation of the error contributor  $\therefore$

$\sigma_y$  = expected standard deviation (uncertainty) of error contributor “ $y$ ”



### 3.3.5 Error Budget

The Error Budgets for Cloud Top Parameters are provided in Raytheon VIIRS Error Budget, Version 3 (Y3249). Put a summary page of error budget here (some section of CTPParameters error budget document)

## 3.4 ALGORITHM SENSITIVITY STUDIES

Algorithm sensitivity studies were conducted in earlier stages of the project to determine the impact of individual sensor error contributions on algorithm performance. A number of standard scenes were used to support these studies. These studies led to the initial estimates of sensor performance required to meet or exceed SRD requirements.

The studies were divided into three categories: calibration, instrument noise, and ancillary data errors. Examples of each follow.

### 3.4.1 Calibration Errors

Calibration errors refer to errors in EDR parameter retrievals due to uncompensated biases in radiance measurements. These particular studies address biases that would cause all thermal, and separately, all solar channels to be biased in the same direction. That is, IR and solar biases are independent. These types of biases occur when the emissivity of the on-board blackbody or the reflectivity of the on-board solar diffuser drifts over time. In these studies, the impact of biases on long-term stability and absolute radiometric accuracy are examined. To examine absolute radiometric accuracy, we use the measurement accuracy metric defined in the SRD:

$$\beta = |\mu(\gamma\%) - x_T| \quad (5)$$

where

$\mu(\gamma\%)$  is the average parameter retrieval for the same truth value with an  $\gamma\%$  radiance perturbation

where

$$\mu = \sum_N x_i / N \quad (6)$$

$x_T$  is the truth value of the parameter

$N$  is the number of values included in the average.

To examine long-term stability, we define a metric similar to the long-term stability metric defined in the SRD. [Note: the SRD definition of long-term stability treats time series data. The approximate formula that follows treats perturbations as though they were short-term biases in radiance measurements.]

$$\rho = \sum_N |(x_i(\gamma\%) - x_i(-\gamma\%))| / N \quad (7)$$

### 3.4.1.1 Radiometric Accuracy Results

Figures 5a and b show the results for Scenario 4; a US Standard Atmosphere case, nadir satellite view, and with a water cloud inserted between 3 and 4 km. These results demonstrate the effect on retrieved cloud top temperature of biases of 0.1, 0.5, 1 and 2 percent in the 10.8  $\mu\text{m}$  radiance, for a range of cloud effective particle sizes and optical depths. The light grey shading indicates where errors exceed the Measurement Accuracy objective values and the dark grey shading shows where errors exceed the threshold values contained in the SRD for clouds of optical depth greater than 0.1 (TBR). The size of the bias that can be tolerated tends to increase with effective particle size and optical depth; this is typical of the results for other scenarios. For  $r_e = 5$  (a typical size for an altocumulus cloud) and  $\tau = 1$ , we see that the threshold is met at a perturbation of 1 percent and for optical depths greater than 2, perturbations exceeding 2 percent meet threshold.

It is interesting to examine results for typical effective particle sizes for water droplet clouds, which generally occur in the range 4.0 to 5.0  $\mu\text{m}$  (see Liou, 1992, p. 187). Table 7 shows the bias above which threshold measurement accuracy is exceeded, for  $r_e = 5$  and for  $\tau = 1$  and 10 for cloud top height, temperature, and pressure. Biases range from about 1 to 5 percent, in general.

### 3.4.1.2 Radiometric Stability Results

Figure 6 provides results of the computation of the long-term stability metric, as a function of optical depth and effective particle size for scenario 4. The size of the bias that can be tolerated tends to increase with effective particle size and optical depth; this is typical of the results for other scenarios. Biases between 0.1 and 0.5 percent will meet threshold requirements for most optical depths and effective particle sizes. For  $r_e = 5$  (typical altocumulus cloud) biases exceeding 0.5 percent can be tolerated for optical depths exceeding 4.

It is interesting to examine results for typical effective particle sizes for water droplet clouds which generally occur in the range 4.0 to 5.0  $\mu\text{m}$  (see Liou, 1992, pg. 187). Table 8 shows the bias above which threshold long-term stability is exceeded for  $r_e = 5$  and for  $\tau = 1$  and 10 for cloud top height, temperature, and pressure. Biases range from about 0.1 to 0.7 percent, in general. The analysis includes mid-latitude and tropical scenarios for nadir and edge-of-scan cases.

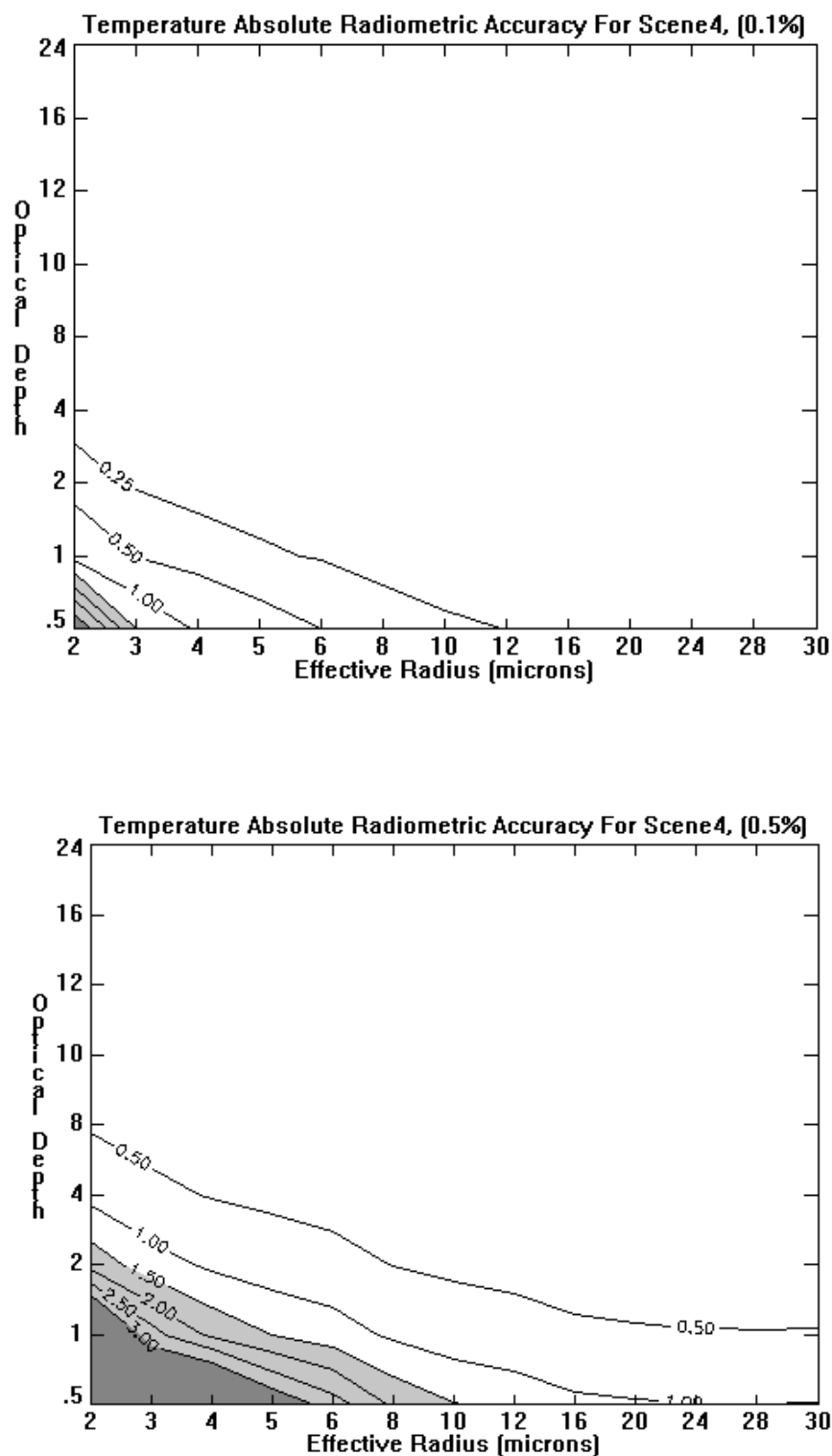


Figure 5a. Radiometric Accuracy results for 0.1% (top) and 0.5% (bottom) perturbations in the 10.8  $\mu\text{m}$  radiances using Scenario 4 and the Window IR algorithm. The measurement accuracy metric is plotted.

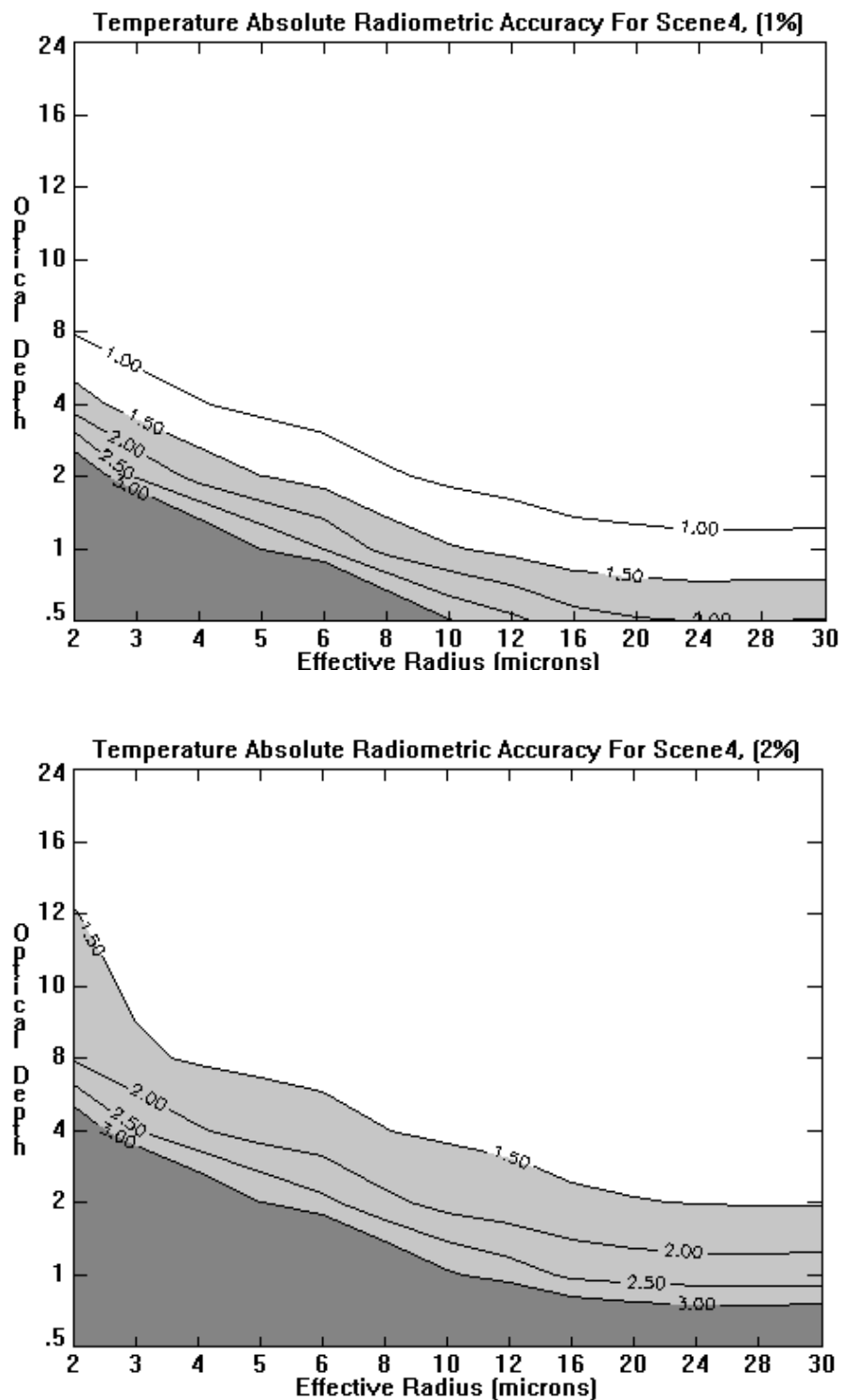


Figure 5b. Radiometric Accuracy results for 1% (top) and 2% (bottom) perturbations in the 10.8  $\mu\text{m}$  radiances using Scenario 4 and the Window IR algorithm. The measurement accuracy metric is plotted.

**Table 7. Bias values (in percent) above which threshold measurement accuracy is exceeded for water droplet clouds, with  $r_e = 5$  and for  $\tau = 1$  and 10.**

EDR Parameter: Cloud Top Height, Temperature, and Pressure  
 Sensor Parameter: Radiometric Accuracy  
 Algorithm: Window IR  
 Effective Radius: Effective Radius = 5  $\mu\text{m}$

Scene	Scene Description	Height		Temperature		Pressure	
		$\tau = 10$	$\tau = 1$	$\tau = 10$	$\tau = 1$	$\tau = 10$	$\tau = 1$
4	Water Cloud (4/1km), US Standard Veg., $\theta = 0$ , $\theta_0 = \text{Night}$	5%	5%	1%	4%	1.5%	5%
7	Water Cloud (4/1km), US Standard Veg., $\theta = 40$ , $\theta_0 = \text{Night}$	5%	5%	1.1%	4%	2%	5%
8	Water Cloud (7/1km), Tropical Veg., $\theta = 0$ , $\theta_0 = \text{Night}$	5%	5%	0.4%	2.5%	5%	5%
17	Water Cloud (4/1km), US Standard Veg., $\theta = 55$ , $\theta_0 = \text{Night}$	5%	5%	2%	4%	5%	5%
18	Water Cloud (7/1km), Tropical Veg., $\theta = 40$ , $\theta_0 = \text{Night}$	5%	5%	0.75%	4%	5%	5%
19	Water Cloud (7/1km), Tropical Veg., $\theta = 55$ , $\theta_0 = \text{Night}$	5%	5%	2%	4.5%	5 %	5%

**Table 8. Bias values (in percent) above which threshold long-term stability is exceeded for water droplet clouds with  $r_e = 5$  and for  $\tau = 1$  and 10.**

EDR Parameter: Cloud Top Height, Temperature, and Pressure  
 Sensor Parameter: Radiometric Stability  
 Algorithm: Window IR  
 Effective Radius: Effective Radius = 5  $\mu\text{m}$

Scene	Scene Description	Height		Temperature		Pressure	
		$\tau = 10$	$\tau = 1$	$\tau = 10$	$\tau = 1$	$\tau = 10$	$\tau = 1$
4	Water Cloud (4/1km), US Standard Veg., $\theta = 0$ , $\theta_0 = \text{Night}$	0.2%	0.7%	0.1%	0.5%	< 0.1%	0.3%
7	Water Cloud (4/1km), US Standard Veg., $\theta = 40$ , $\theta_0 = \text{Night}$	0.3%	0.75%	0.2%	0.6%	< 0.1%	0.3%
8	Water Cloud (7/1km), Tropical Veg., $\theta = 0$ , $\theta_0 = \text{Night}$	0.1%	0.6%	< 0.1%	0.3%	< 0.1%	0.3%
17	Water Cloud (4/1km), US Standard Veg., $\theta = 55$ , $\theta_0 = \text{Night}$	0.4%	0.75%	0.3%	0.7%	0.15%	0.4%
18	Water Cloud (7/1km), Tropical Veg., $\theta = 40$ , $\theta_0 = \text{Night}$	0.2%	0.7%	0.15%	0.6%	< 0.1%	0.3%
19	Water Cloud (7/1km), Tropical Veg., $\theta = 55$ , $\theta_0 = \text{Night}$	0.4%	0.7%	0.3%	0.7%	0.15%	0.3%

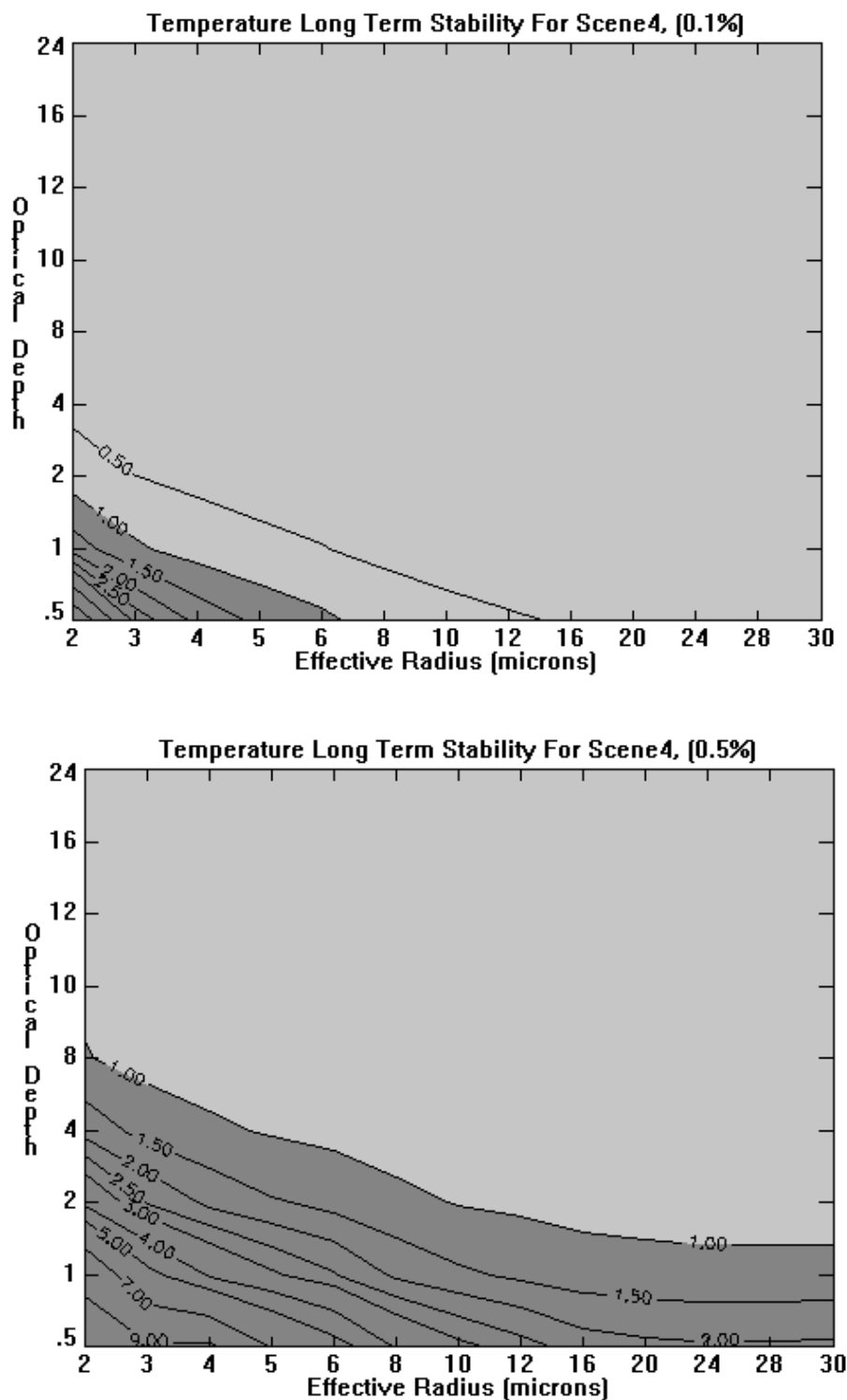


Figure 6. Radiometric Stability results for 0.1% (top) and 0.5% (bottom) perturbations of the 10.8  $\mu\text{m}$  radiances using Scenario 4 and the Window IR algorithm. The long-term stability metric is plotted.

### 3.4.2 Instrument Noise

Instrument noise refers to random noise introduced into the measured radiances by the VIIRS instrument. It is assumed that the noise is uncorrelated in time, from pixel-to-pixel, and across bands. Instrument noise is being investigated through application of seven noise models provided by RSBR (Raytheon Santa Barbara Research). The noise is modeled using a Gaussian distribution, with mean and standard deviation dependent on the waveband and magnitude of radiance. The noise models are numbered 1 through 7, with noise increasing with model number.

Two metrics were applied to investigate the effect of instrument noise on EDR retrieval accuracy: measurement accuracy and measurement precision. For these experiments, the measurement accuracy metric was applied as follows:

$$\beta = |\mu - x_T| \quad (8)$$

where symbols are defined as in Section 3.4.1. For these tests, the mean was developed by randomly adding noise 32 times to the unperturbed radiance value(s) used by the retrieval algorithms. The perturbed radiances were then processed through the retrieval algorithm and the measurement accuracy metric computed. This process was repeated for each noise model.

The measurement precision metric is the standard deviation of the retrieved values, relative to the mean of the retrieval values, with the same truth-value for all retrievals.

$$\sigma = \sqrt{\sum_N (x_i - \mu)^2 / (N - 1)} \quad (9)$$

If we assume that the response of the EDR retrieval algorithm is linear for small radiance perturbations, we can see that the measurement accuracy metric should be insensitive to noise and that the precision metric should be sensitive to noise. This was found to be the case for all but the largest noise models (i.e., noise models 6 and 7).

Figures 7 a-f show contour plots of measurement accuracy, and Figures 8 a-f show measurement precision results for a range of optical depths and effective particle sizes for noise models 1 through 6. The results are for Scenario 4, which is a U.S. Standard Atmosphere case, nadir satellite view, with a water cloud inserted between 3 and 4 km in altitude. In these plots, the light gray shaded regions are regions where the objective is exceeded and the dark gray shaded regions are regions where the threshold is exceeded. It is obvious that measurement accuracy meets both threshold and objective up to noise models 5 and 6, respectively. This was an expected result. Measurement accuracy results for other scenarios are consistent with these findings; therefore, no further instrument noise measurement accuracy results will be shown. On the other hand, measurement precision is affected by instrument noise. The shaded regions expand from the lower left portion of the figures (small optical depth and effective particle size) as instrument noise increases, beginning with noise model 3. These plots indicated that the threshold measurement precision is met for noise model < 5 for virtually all  $r_e$  and  $\tau > 1$ , and the objective is met for noise model < 3 for most  $r_e$  and  $\tau > 1$ .

Figure 9 shows measurement precision results for Scenario 2, a cirrus case. Again, this case is for the U.S. Standard atmosphere, nadir view, and the cirrus cloud is between 9 and 10 km in

altitude. For these plots, the results for all effective particle sizes were aggregated and the precision is depicted as a function of optical depth. Note that the measurement precision meets threshold for most noise models for optical depths greater than about 0.5; the threshold is met for noise model < 5 for  $\tau > 0.125$ .

It is interesting to examine results for typical effective particle sizes for water droplet clouds which generally occur in the range 4.0 to 5.0  $\mu\text{m}$  (see Liou, 1992, pg. 187). Table 9 shows the noise model above which threshold measurement precision is exceeded for  $r_e = 5$  and for  $\tau = 1$  and 10 for cloud top height, temperature, and pressure. In general, noise models 4, 5, and 6 are acceptable. (It should be noted that recent flowdown analyses have indicated that noise model 3 might be more appropriate when other contributors to the error budget are considered, particularly for small optical depths.). The analysis includes mid-latitude and tropical scenarios for nadir and edge-of-scan cases.

**Table 9. Noise model above which threshold measurement precision is exceeded for water droplet clouds with  $r_e = 5$  and for  $\tau = 1$  and 10.**

EDR Parameter: Cloud Top Height, Temperature, and Pressure  
 Sensor Parameter: Radiometric Noise  
 Algorithm: Window IR  
 Effective Radius: Effective Radius = 5  $\mu\text{m}$

Scene	Scene Description	Height		Temperature		Pressure	
		$\tau = 1$	$\tau = 10$	$\tau = 1$	$\tau = 10$	$\tau = 1$	$\tau = 10$
4	Water Cloud (4/1km), US Standard Veg., $\theta = 0$ , $\theta_0 = \text{Night}$	Model 4	Model 5	Model 4	Model 5	Model 5	Model 5
7	Water Cloud (4/1km), US Standard Veg., $\theta = 40$ , $\theta_0 = \text{Night}$	Model 4	Model 5	Model 4	Model 5	Model 5	Model 5
8	Water Cloud (7/1km), Tropical Veg., $\theta = 0$ , $\theta_0 = \text{Night}$	Model 4	Model 5	Model 3	Model 5	Model 5	Model 6
17	Water Cloud (4/1km), US Standard Veg., $\theta = 55$ , $\theta_0 = \text{Night}$	Model 5	Model 5	Model 5	Model 5	Model 5	Model 5
18	Water Cloud (7/1km), Tropical Veg., $\theta = 40$ , $\theta_0 = \text{Night}$	Model 4	Model 5	Model 4	Model 5	Model 5	Model 6
19	Water Cloud (7/1km), Tropical Veg., $\theta = 55$ , $\theta_0 = \text{Night}$	Model 6	Model 5	Model 5	Model 5	Model 6	Model 6



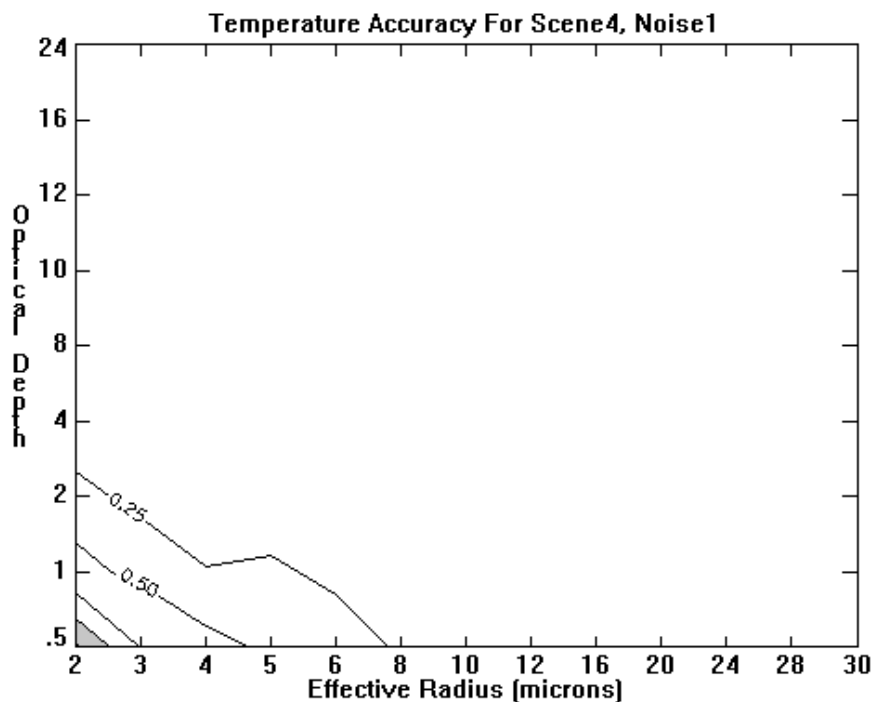


Figure 7a. Instrument noise contour plot for measurement accuracy. Scenario 4, Model 1.

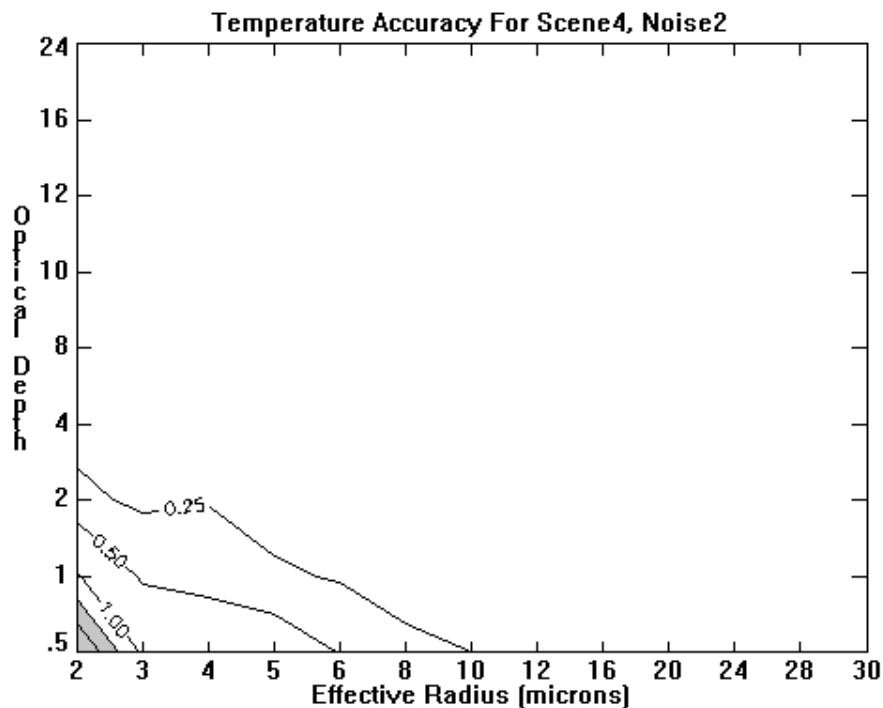


Figure 7b. Instrument noise contour plot for measurement accuracy. Scenario 4, Model 2.

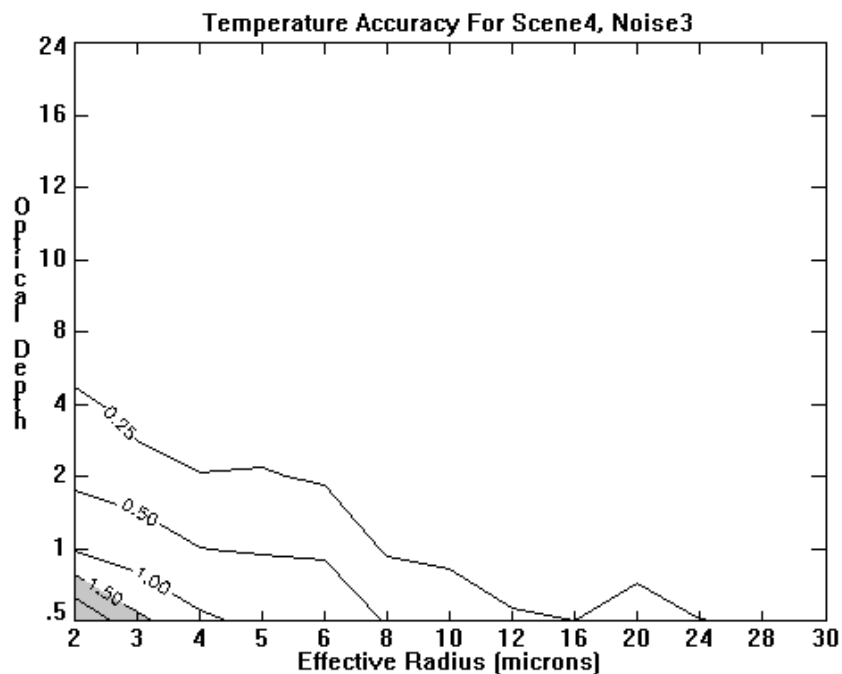


Figure 7c. Instrument noise contour plot for measurement accuracy. Scenario 4, Model 3.

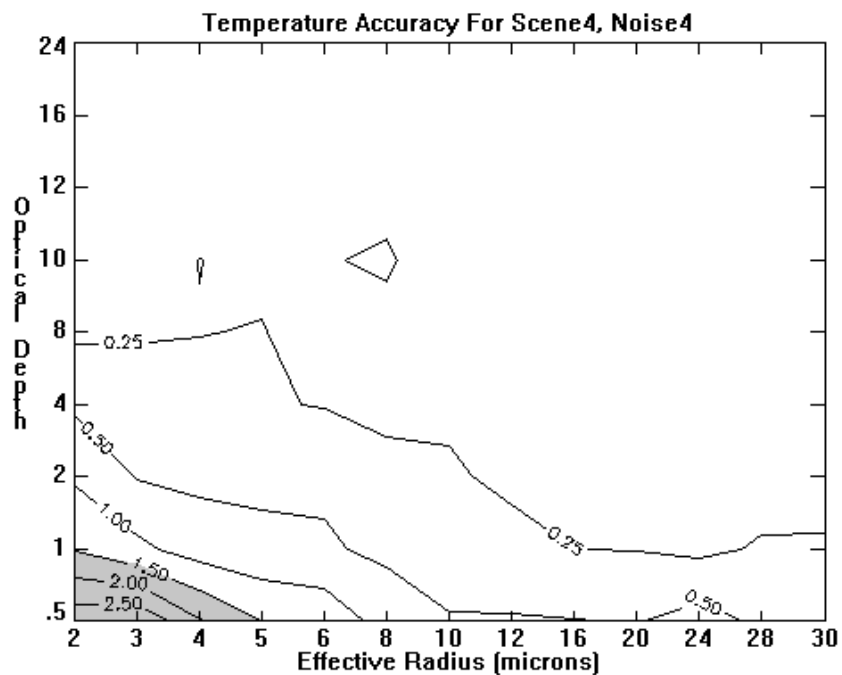


Figure 7d. Instrument noise contour plot for measurement accuracy. Scenario 4, Model 4.

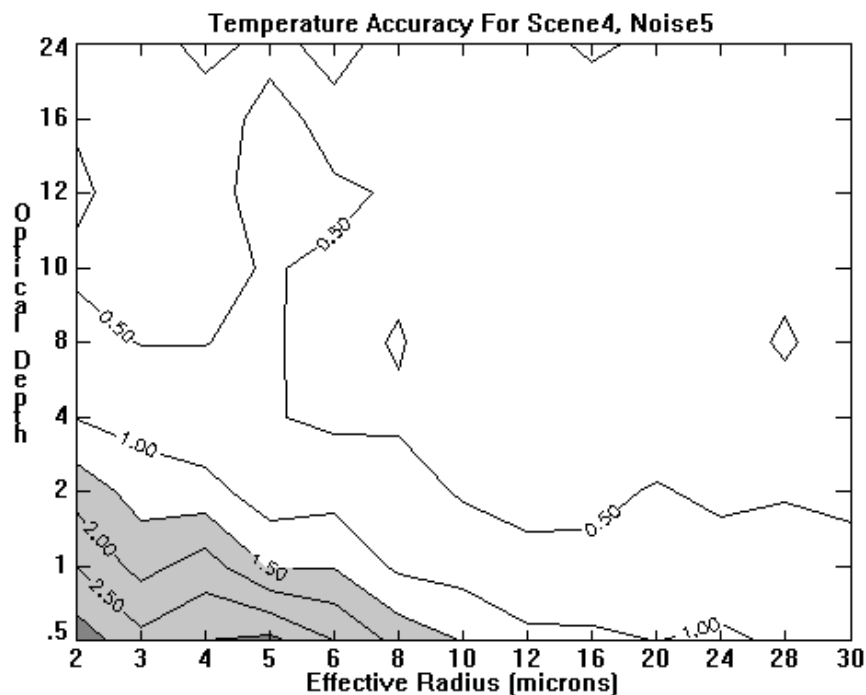


Figure 7e. Instrument noise contour plot for measurement accuracy. Scenario 4, Model 5.

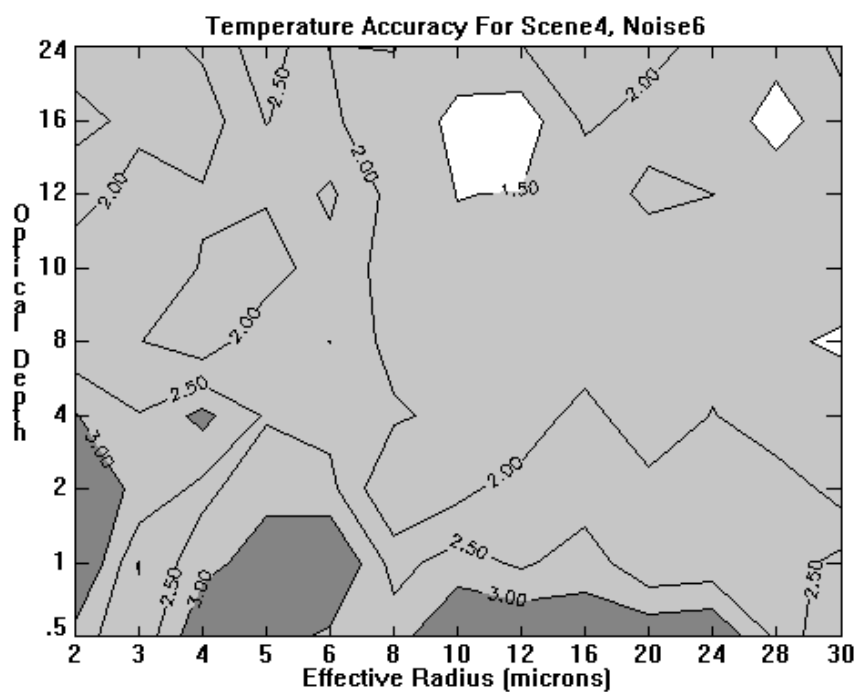


Figure 7f. Instrument noise contour plot for measurement accuracy. Scenario 4, Model 6.

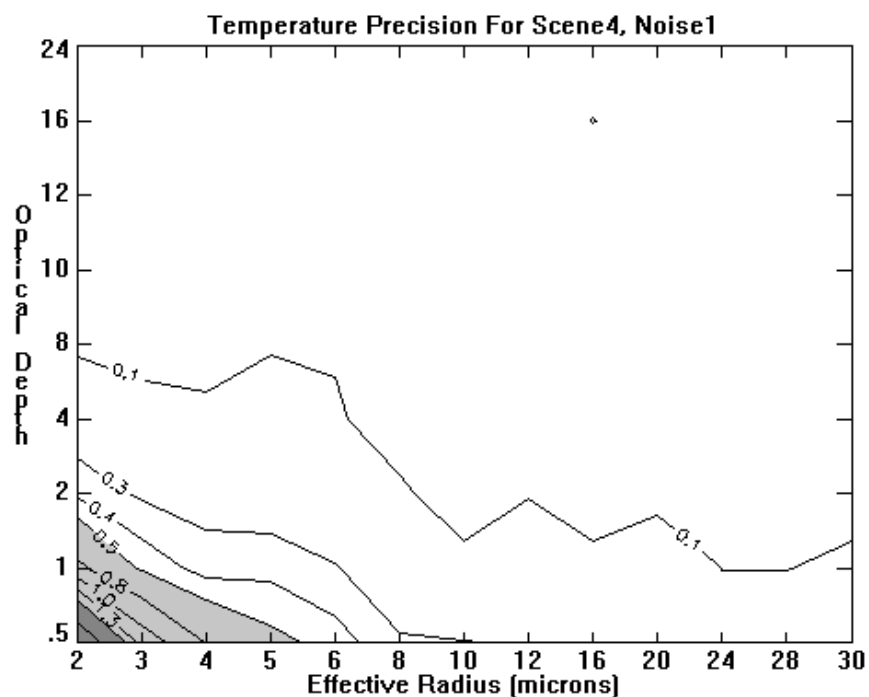


Figure 8a. Instrument noise measurement precision. Scenario 4, Model 1.

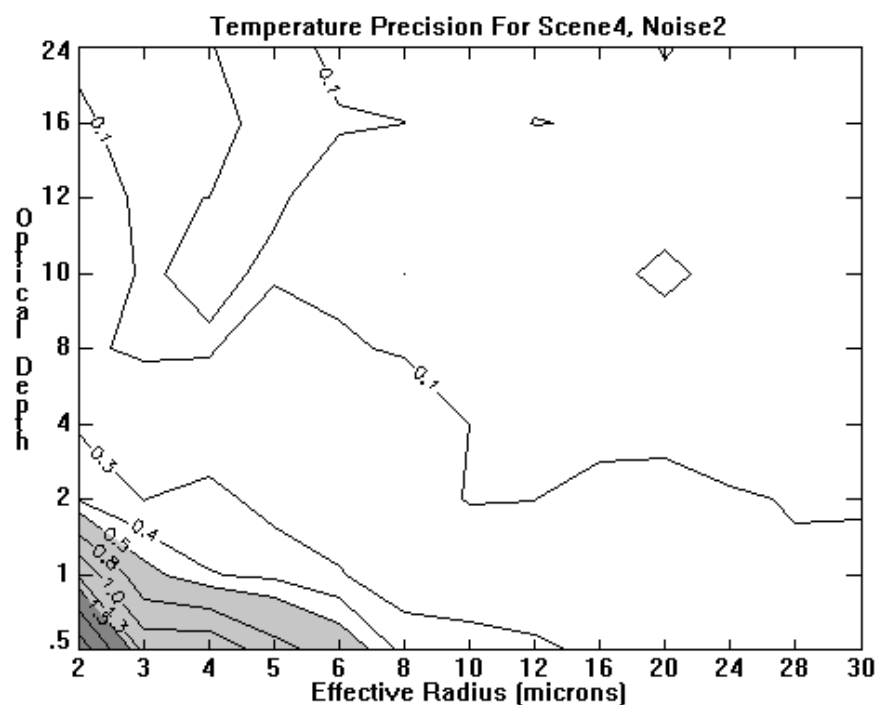


Figure 8b. Instrument noise measurement precision. Scenario 4, Model 2.

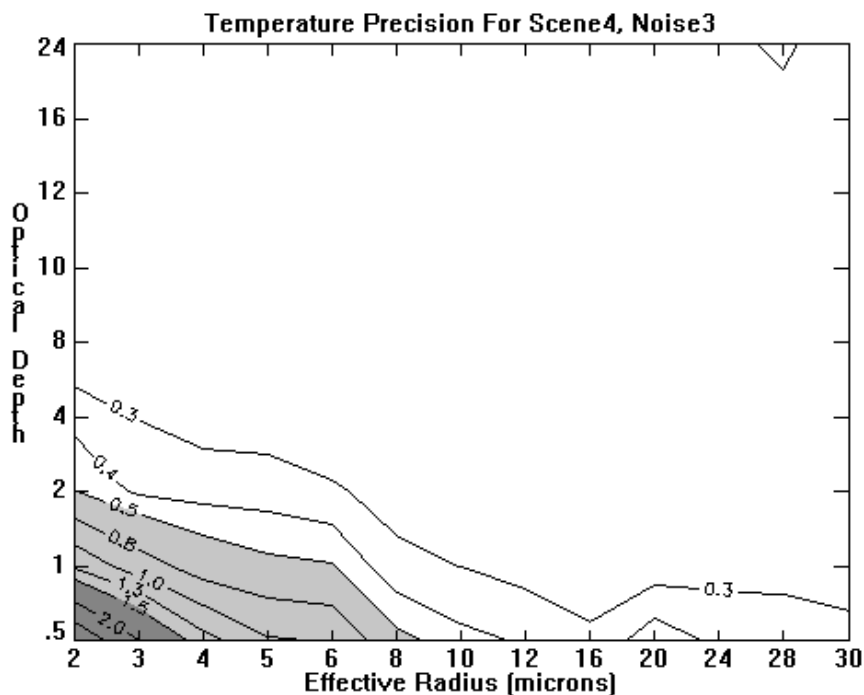


Figure 8c. Instrument noise measurement precision. Scenario 4, Model 3.

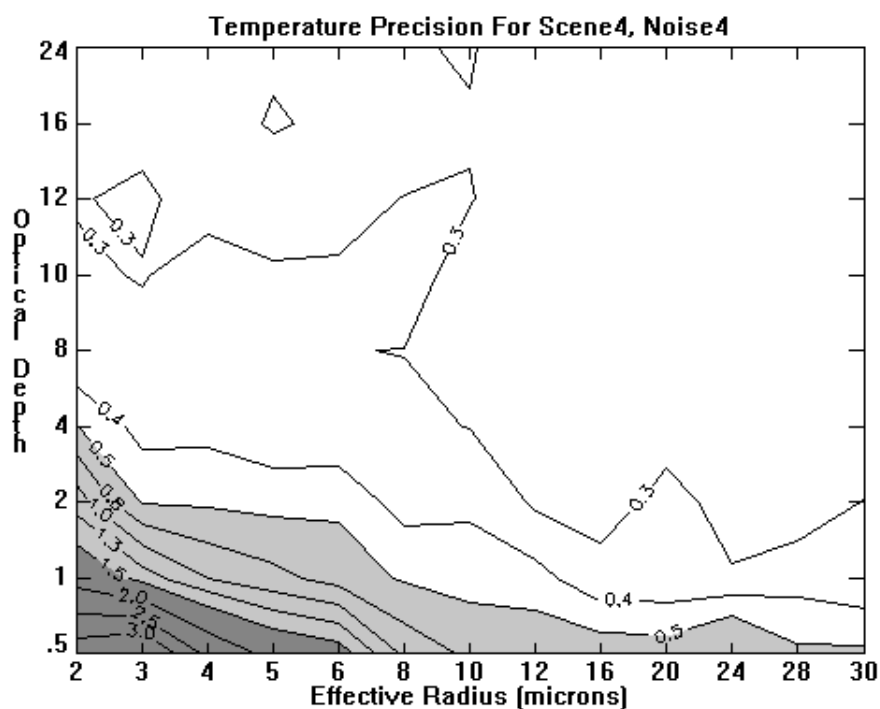


Figure 8d. Instrument noise measurement precision. Scenario 4, Model 4.

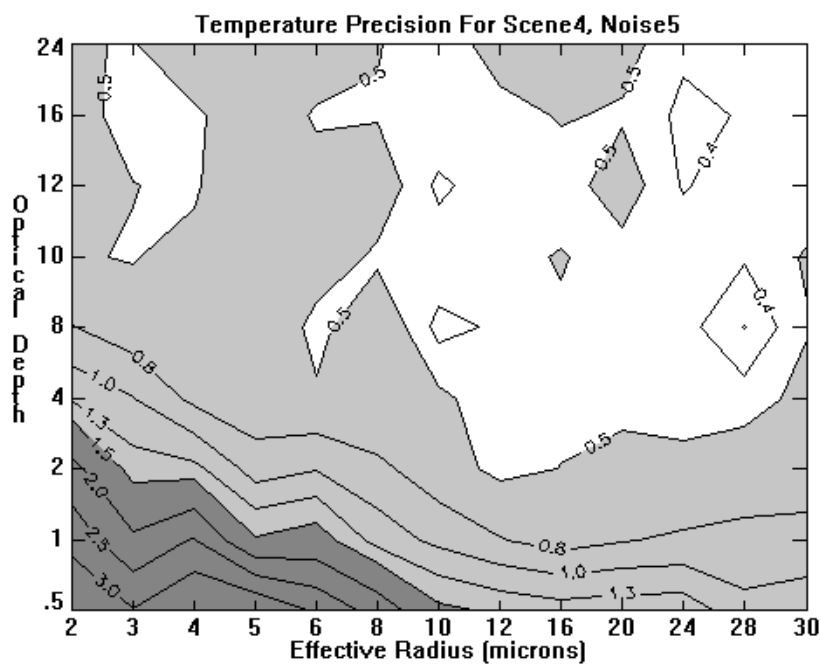


Figure 8e. Instrument noise measurement precision. Scenario 4, Model 5.

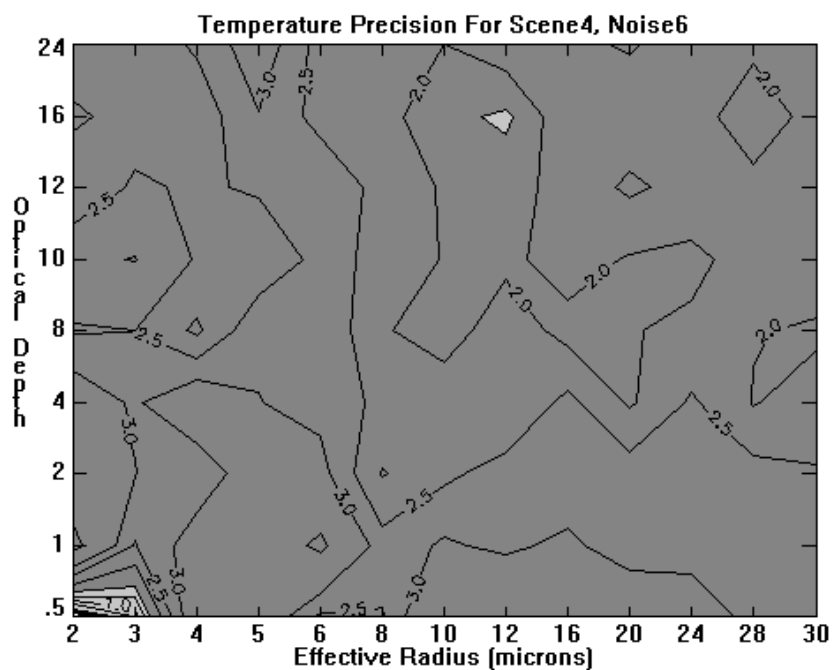


Figure 8f. Instrument noise measurement precision. Scenario 4, Model 6.

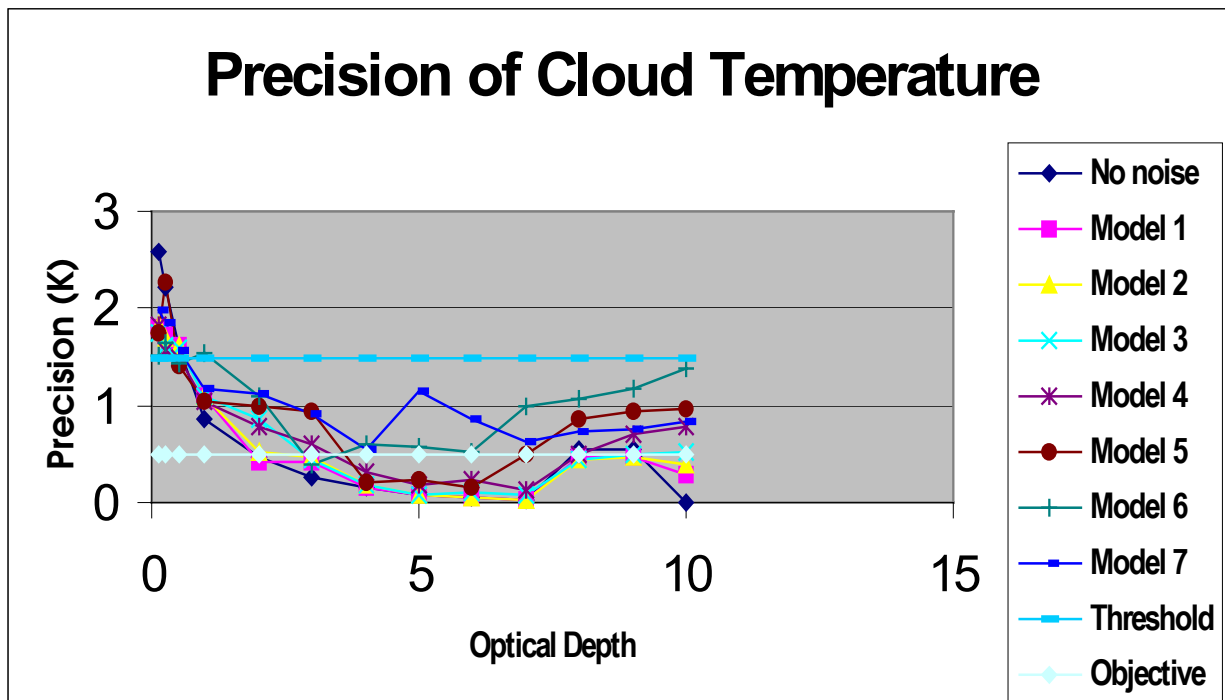


Figure 9. Instrument Noise Measurement Precision Results. Scenario 2.

### 3.4.3 Ancillary Data

The identification and contribution to performance of uncertainties in ancillary data and other sensor error sources are addressed in the error budget studies in Sections 3.3.4 and 3.3.5.

## 3.5 PRACTICAL CONSIDERATIONS

The discussions in this section apply mainly to the Window IR and cloud top parameter interpolation algorithms. See Ou *et al.* (2000) for a discussion of the IR Cirrus and Water Cloud Parameter Retrieval Algorithms, which estimate cloud top temperature for cirrus (ice) clouds (day and night) and water clouds at night.

### 3.5.1 Numerical Computation Considerations

A practical issue to be resolved involves the radiative transfer analysis that must be performed to support the Window IR solution. The approach requires up to N radiative transfer solutions for the Specified Environmental Scenario and for a cloud layer positioned in one-kilometer steps from the ground to N kilometers in altitude. The retrieved cloud top altitude is the one for which the solution and VIIRS 10.8  $\mu\text{m}$  radiance measurement best match. A comprehensive radiance look-up table (LUT) is required to apply the algorithm operationally. In the LUT approach, radiance tables are pre-computed and accessed each time a retrieval is performed. During VIIRS

algorithm development phase II optimal methods to identify the appropriate look-up table will be developed and the tables must extend over the complete operational range of Environmental Scenarios at sufficient resolution in parameter space to meet retrieval accuracy requirements. Alternative on-line radiance calculation will also be tested to see it still can meet the timely processing requirement for EDR generation.

### 3.5.2 Programming and Procedural Considerations

#### 3.5.2.1 Programming Considerations

The Window IR and interpolation algorithms are written in the C programming language and should be easily transferrable to other computation environments.

#### 3.5.2.2 Procedural Considerations

Table 10 provides an outline of the procedure for determining cloud top parameters.

**Table 10. Cloud Top Parameter Retrieval Procedure**

Step	Description
1	Obtain VIIRS data: radiances, sun-sensor geometry, and cloud mask and cloud phase (ice or water cloud) results.
2	Obtain ancillary data required by algorithms.
3A	Ice cloud. Execute UCLA IR cirrus parameter retrieval algorithm. See Ou <i>et al.</i> (2000). Go to step 4A.
3B	Water cloud Daytime. Initialize $\tau$ and $r_e$ . Execute Window IR algorithm. Go to step 4B.
3C	Water cloud Nighttime. Execute UCLA IR water parameter retrieval algorithm. See Ou <i>et al.</i> (2000). Go to step 4A.
4A	UCLA Algorithm. Execute Interpolation Algorithm to obtain cloud top height and pressure from cloud top temperature. Go to step 5.
4B	Window IR Algorithm. Execute Interpolation Algorithm to obtain cloud top temperature and pressure from cloud top height.
5	Store "final" values of cloud top parameters and quality flags in database for aggregation to HCS and processing by other EDRs.

### 3.5.3 Configuration of Retrievals

As previously indicated, the retrieval of cloud top parameters will follow execution of the VIIRS Cloud Mask algorithm, which also computes cloud phase for each pixel. For ice clouds, the UCLA IR cirrus parameter retrieval algorithm will be executed to determine cloud top temperature for ice clouds, day or night. This cloud top temperature will be used to determine other cloud top parameters with the use of sounding (temperature versus height and pressure) data. For water clouds during night time, the UCLA IR water cloud parameter retrieval algorithm will be executed to determine cloud top temperature for water clouds. For water clouds during day time, the Window IR algorithm would be executed. Prior to executing the Window IR algorithm, the UCLA solar retrieval algorithm for optical properties for water clouds will be executed to provide effective particle size and optical thickness information needed by the Window IR algorithm. These two algorithms could also be executed iteratively to determine the cloud top temperature and optical properties that are most consistent with the measurements. The resulting cloud height will be used to determine the remaining two cloud top parameters.



### 3.5.4 Quality Assessment and Diagnostics

The assessment of the quality of retrievals will fall into four categories: Sensor Parameters; Environmental Scenario; Cloud Scenario; and Ancillary Data. Experience gained through simulations, and eventually by validation, will be captured and used to assess the quality of retrievals and provide guidance to the users of these products in the form of data quality flags. A list of parameters or situations that may influence data quality follows.

- *Sensor Parameters.* The Qualities of sensor data include:
  - Sensor noise.
  - Radiance calibration.
  - Geolocation.
  - MTF
  - Band-to-Band registration.
- *Environmental Scenario.* Particulars of the environmental scenario that may affect retrieval accuracy include:
  - Values of Environmental Parameters. Sensitivity studies and flowdown indicate that retrieval accuracy is a function of the particular values of some environmental parameters (e.g, surface temperature, surface emissivity, sounding data).
  - Atmospheric inversion/isothermal identified in sounding.
  - Atmospheric water vapor absorption correction can improve over-estimation of cloud top height (cloud estimated too high)
- *Cloud Scenario.* The qualities or values of other cloud parameters that may affect retrieval accuracy include:
  - Cloud optical depth. Flowdown results show that retrieval accuracy can be a function of optical depth.
  - Cloud effective particle size. Flowdown results show that retrieval accuracy can be a function of effective particle size.
  - Existence of multilayer clouds. Multilayer clouds are difficult to identify and have an impact on radiance measurements. The primary problem is when a thin cloud overlays a lower cloud layer. Therefore, multi-layer clouds will affect retrievals when a single layer cloud is assumed in the radiative transfer analysis or retrieval algorithm and a multi-layer cloud actually exists within the field-of-view.

- Satellite viewing geometry. Flowdown results show some sensitivity to satellite view geometry.
- Solar position. Solar position influences UCLA IR cirrus parameter retrievals during daytime.
- Non-overcast cloudy pixel. Sub-pixel cloud results under-estimation of cloud top height.
- *Ancillary Data*
  - In general, the quality of ancillary data affects the quality of retrievals. This has been explored in the Error Budget studies.

### 3.5.5 Exception Handling

We define “exception handling” as the procedure for handling missing or degraded data or a degraded processing environment.

#### 3.5.5.1 Missing/Degraded Data

Table 11 lists VIIRS and ancillary data, potential primary and secondary sources of these data, and whether these data are essential or nonessential. We define “essential data” to mean data that are absolutely necessary to meet EDR threshold requirements, and “nonessential data” as data that improve retrievals.

#### 3.5.5.2 Degraded Processing Environment

The most resource-intensive task associated with these algorithms involves executing the radiative transfer model. As indicated previously (Sections 3.3.2.1 and 3.5.1), this may be done “on the fly,” or pre-computed radiance look-up tables may be consulted. An interesting compromise would be to build the look-up tables as part of the “operational processing.” The radiance results for new scenarios would be archived. If the scenario occurs again (within some tolerance), the radiative transfer model would not be rerun; rather, the previously generated look-up table would be used. This scheme would allow interpolation between look-up tables, as is required for any look-up table solution. It is very likely that within a few months of processing (perhaps spread out over the year), a very representative set of look-up tables will have been developed. At the very least, these tables would be the source of radiance data in degraded processing mode; at most they would be the primary source of radiance data.

**Table 11. Data used by retrieval algorithms, whether the data are essential or nonessential, and primary, secondary, and tertiary data sources.**

Data Type	Description	Essential/ Nonessential	Potential Source*
VIIRS Radiances	0.672, 3.70, and 10.8 $\mu\text{m}$ radiances	Essential	1: VIIRS 2: None
Sensor Viewing Geometry	Sensor zenith and azimuth angles for each pixel	Essential	1: VIIRS Calibrated TOA SDR 2: Modeled using satellite ephemeris data
Solar Geometry	Solar zenith and azimuth angles for each pixel	Essential during daytime	1: VIIRS Calibrated TOA SDR 2: Modeled using previous satellite ephemeris data
Cloud Mask	Cloud/no cloud for each pixel	Essential	1: VIIRS Cloud Mask algorithm 2: Cloud/no cloud based on simple thresholding
Cloud Phase	Ice cloud or water cloud flag	Essential	1: VIIRS Cloud Mask algorithm 2: CMIS IWC and CLW data
Cloud Optical Depth	Pixel-level optical depth of ice or water cloud	Essential for Window IR during daytime	1: VIIRS Cloud Optical Depth EDR algorithm 2: Default values
Cloud Effective Particle Size	Pixel-level effective particle size of ice or water cloud	Essential for Window IR during daytime)	1: VIIRS Cloud Effective Particle Size EDR algorithm 2: Default values
Atmospheric Sounding	Atmospheric temperature and relative humidity as functions of pressure and height	Essential	1: NCEP re-analysis 2: CMIS sounding data 3: CrIS sounding data
Surface Emissivity	In-band emissivity of Earth's surface	Essential	1: Emissivity from Spectral Library associated with terrain category VIIRS Surface Types- Olson IP 2: Same, but using database other than VIIRS
Surface Skin Temperature	Skin temperature associated with pixel region	Essential	1: NCEP re-analysis and forecast 2: VIIRS Land Surface Temperature EDR and Sea Surface Temperature EDR
*1 = Primary Potential Source      *2 = Secondary Potential Source      *3 = Tertiary Potential Source			

### 3.6 ALGORITHM VALIDATION

The Cloud Integrated Product Team (IPT) has or will have access to a number of data sources that could be used to validate the Cloud Top Parameter retrieval algorithms. These sources include the following:

- Radiance data collected by the MODIS Airborne Simulator (MAS), with cloud tops

determined from the on-board lidar data.

- MODIS data when available, together with the use of data from associated retrieval algorithm validation campaigns.

The validation effort should be able to take advantage of past and planned cloud field campaigns (such as FIRE-I, FIRE-II, ARM Spring 2000, Fire Tropical 2002/2003, and the Terra validation studies). Regardless of the data used, it is essential that the data sets include reliable radiance data at or very near the proposed VIIRS wave bands, all required ancillary data, and an accurate description of the associated cloud parameters (type, base, height, optical properties, etc.) for ground truth. During phase II at least one MODIS data will be used to test cloud top parameter processing performance and provide these analyses in version 5 ATBD.

### **3.7 ALGORITHM DEVELOPMENT SCHEDULE**

Phase II algorithm development will include the followings:

3.7.1 UCLA and TASC water cloud top height retrieval comparison

3.7.2 Non-overcast pixel cloud top parameters retrieval analysis

3.7.3 Implement water vapor absorpition correction for 10.8 micron channel before performing Window IR algorithm

3.7.4 Implement multiplelayer cloud retrieval algorithm

3.7.5 Validate UCLA/TASC cloud top parameter retrieval algorithm using Terra MODIS data

3.7.6 Revise/update ATBD to reflect all phase II changes and enhanced algorithm performance

## 4.0 ASSUMPTIONS AND LIMITATIONS

### 4.1 ASSUMPTIONS

The major assumptions listed below relate to the Window IR and Cloud Top Parameter Interpolation Algorithms. See Ou *et al.* (2000) for a description of the assumptions made in the UCLA Cloud Parameter Retrieval Algorithm.

- The retrieval algorithm is based on plane-parallel radiative transfer theory. Horizontal inhomogeneities in cloud and environmental parameters and their effects on radiative transfer are not modeled.
- At this time, multilayer cloud conditions are not modeled in the radiative transfer solution. Degraded performance is expected when multilayer clouds are present within the same pixel.
- It is assumed that the atmosphere is in thermodynamic equilibrium and that the hydrostatic approximation applies.
- It is assumed that the optical properties of water droplet clouds are not sensitive to the exact shape of the particle size distribution.
- It is assumed that no sub-pixel clouds exist.
- It is assumed that 10.8 micron channel is not affected by aerosol absorption.

### 4.2 LIMITATIONS

No major limitations have yet been identified for the Window IR and cloud top parameter Interpolation Algorithms. The algorithms are applicable both day and night, and results indicate accurate retrievals are possible over the full range of viewing geometries. See Ou, *et al.* (2000) for a description of the limitations of the UCLA Cloud Parameter Retrieval Algorithm. We do expect degraded performance when multilayer and sub-pixel clouds are present within pixels and when a temperature inversion/isothermal is present in the atmosphere. The impacts of these conditions on retrieval accuracy have not yet been quantified.



## 5.0 REFERENCES

- Chylek, P, P. Damiano, and E.P. Shettle (1992). Infrared emittance of water clouds. *Journal of the Atmospheric Sciences*, Vol. 49, No. 16, 15 August 1992.
- Liou, K.N. (1992). *Radiation and Cloud Processes in the Atmosphere: Theory, observation, and modeling*. New York: Oxford University Press.
- Menzel, P. and K. Strabala (1997). Cloud Top properties and cloud phase algorithm theoretical basis document. MODIS Algorithm Theoretical Basis Document No. ATBD-MOD-04, October 1997 (version 5).
- Ou, S.C., K.N. Liou, and Y. Takano (2000). VIIRS cloud optical depth and cloud effective particle size algorithm theoretical basis document. PR-08923-04-09, Version 3. Raytheon STX Cloud Integrated Product Team.
- Raytheon VIIRS Error Budget, Version 3 (Y3249)
- SRD. Visible/Infrared Imager/Radiometer Suite (VIIRS) Sensor Requirements Document (SRD) for National Polar-orbiting Operational Environmental Satellite System (NPOESS) spacecraft and sensors. Associate Directorate for Acquisition NPOESS Integrated Program Office. Version 2, Revision a, 4 November 1999. F04701-97-C-0028.
- Rossow, W.B., L.C. Garder, P.J. Lu, and A.W. Walker, 1991: International Satellite Cloud Climatology Project (ISCCP) Documentation of Cloud Data. WMO/TD-No. 266, World Meteorological Organization, 76 pp.